CENTRE NATIONAL
DE LA RECHERCHE
SCIENTIFIQUE

Laboratoire
Léon Brillouin

cea

SUPERCONDUCTIVITY AND MAGNETISM

SUPERCONDUCTIVITY AND MAGNETISM

Over the years, neutron scattering has imposed itself as a prominent tool for studying the microscopic mechanisms of magnetism in solids. In the context of the emergence of powerful new techniques such as real-space imaging, high-field NMR, or magnetic x-ray scattering, its contribution remains central because, as problems of growing complexity can be tackled, it becomes essential to fully exploit complementarities between different probes. Indeed, the installation of the new synchrotron source SOLEIL in the close neighborhood of LLB is stimulating projects for future collaborations in the field of magnetism. The comparison of spin and charge excitation spectra, for example, can be expected to be one of the keys to understanding the properties of strongly correlated electrons and the occurrence of unconventional superconductivity. Even before the first x-ray beams have been produced, two joint LLB-SOLEIL workshops in this field, *Magnetism and Nanostructures* (May 2005) and *Strongly Correlated Electrons* (June 2006), have already been held.

This part of the Report describes recent neutron work of magnetism and superconductivity in different classes of materials, from transition-metal oxides and lanthanide compounds with strong electron correlations to frustrated magnetic systems, molecular magnets and photomagnetism (other aspects of magnetism, more closely related to structures or phase transitions, are covered in the corresponding chapter). After giving an overview of the salient results, and placing them in perspective with the current trends of research in each field, selected studies are presented in the form of self-contained "highlights", followed by shorter contributions ("clips") intended to give a snapshot at one particularly interesting piece of data.

Whereas a majority of these results have been obtained on the pool of neutron spectrometers available in Saclay, a growing number of LLB scientists frequently carry out experiments on other neutron sources (ILL, FRMII, ISIS, PSI, NIST, etc.) as part of their own research programs, in order to make optimal use of the specificities of each instrument.

A - Strongly correlated electrons

Several families of 3*d* element oxides are known to exhibit most unusual electronic and magnetic properties, among which "colossal" magnetoresistance (CMR) in manganites or unconventional superconductivity in quasi-2D systems such as in high-T_c cuprates, ruthenates or hydrated cobaltates. In all these systems, strong electronic correlations, as well as the complex interplay between different degrees of freedom (charge, spin, orbital moment, lattice vibrations,…) seem to play a crucial role. Neutron scattering techniques are unique in their ability to reveal spin or orbital magnetic order, to measure spin excitation spectra, or to trace anomalies in lattice dynamics. It is therefore no surprise that the properties of those systems, either static or dynamic, constitute one of the most active fields of research at LLB, like in many other neutron centers.

Heterogeneity in charge distributions, such as charge segregation or charge ordering, is one of the key aspects for understanding the new properties of several families of oxides exhibiting colossal magnetoresistance (CMR), "stripe" structures, etc. In other systems, like Sr_2RuO_4, the electronic and magnetic properties are more indicative of a homogeneous charge distribution (itinerant models), but strong correlations among the carriers remain central to their low-temperature properties, including superconductivity. In the case of high-T_c cuprates, the validity of approaches based on stripes or, alternatively, on a homogeneous itinerant spin-exciton picture, remains controversial. Important new results make it possible to assess the implications of each model in greater detail. Studies on oxides with exotic electronic properties reinforce the interest for the physics taking place close to quantum critical points, which has long been a recurrent question in heavy-fermion systems. The comparison of properties in electron- and hole-doped cuprates is an important aspect of this problem. In relation with the central role played by orbital order in transition metal oxides, quadrupolar degrees of freedom of 4*f* electron states are now being recognized as a main source of novel physical phenomena in rare-earth compounds, among which a number of unconventional long-range order and fluctuations, possibly providing a novel route to superconductivity.

It is worth noting that many of the studies described in this section concern new compounds, for which the possibility to work on large, high-quality single crystals has been crucial. This clearly reflects the key role assumed by material synthesis and crystal growth, and emphasizes the urgent need to reinforce those activities as a basis for the development of forefront programs in solid-state physics at neutron sources and other large facilities.

INHOMOGENEOUS CHARGE STATES : FROM MANGANITES TO CUPRATES

In the 3D manganites $La_{1-x}(Sr,Ca)_xMnO_3$, recent measurements have brought to light the existence of nanoscopic ferromagnetic platelets, which, as can be deduced from their anisotropic coupling, are associated with a low hole density. The magnetic excitations in these nano-objects take the form of stationary waves, which have been observed by inelastic neutron scattering [***H4***, S. Petit]. For the particular composition $x = 1/8$ and for $x = 0.15$, these ferromagnetic clusters become self-organized, leading to a rearrangement of both spin and charge textures. The evolution of the platelets through the metal-insulator transition occurring at $x = 0.175$ is still under study.

Replacing La by Pr in $Pr_{1-x}Ca_xMnO_3$ suppresses the ferromagnetic metallic region in the phase diagram, so that the compound remains insulating at all *x*. There, the interesting evolution is that observed under an applied field of a few tesla, which restores a metallic state. Quantitative analysis of small-angle magnetic neutron scattering in CMR $Pr_{1-x}Ca_xMnO_3$ crystals (for *x* near 0.33) has shown that the magnetic heterogeneities take place at different scales (thesis of D. Sorel, Crismat–LLB)[1]. Applying a field close to the value where the CMR effect is observed causes mesoscopic (200 nm) inhomogeneities of (conducting) ferromagnetic phase to grow within the insulating phase. Nanoscopic inhomogeneities are also present (both as small ferromagnetic clusters inside the antiferromagnetic (AFI) phase and as small *paramagnetic* ones inside the ferromagnetic phase), but they do not exhibit any change under the application of the field.

In the layer compound $La_{2-x}Sr_xMnO_4$ [***H5**, D. Senff*], which does not exhibit giant magnetoresistance properties and remains insulating, a complex spin excitation spectrum has been observed close to the concentration $x = 1/2$. It can be perfectly described by the appearance of zigzag charge lines, resulting from the competition between spin and charge degrees of freedom. The appearance of coupled spin and charge arrangement into stripes has been recognized for quite a long time in another layered system, $La_{2-x}Sr_xNiO_4$. In order to achieve a better understanding of the different parameters controlling spin and charge ordering, neutron scattering studies have been extended to isostructual systems with different transition metals, for instance $La_{2-x}Sr_xCoO_4$ (Ph. D. thesis of M. Zwick, Univ. Cologne).

It has been proposed that stripes could also play a crucial role in the anomalous electronic properties of high-temperature superconductors. There is experimental evidence, based on neutron studies, that static stripes can indeed exist in $La_{2-x}Ba_xCuO_4$ close to $x = 1/8$. Since lattice vibrations involving oxygen atoms can be extremely sensitive to the formation of charge lines, neutron scattering has been used to track phonons anomalies in order to reveal the existence of stripes. Evidence has indeed been found for a softening of the Cu–O bond-stretching mode in the latter compound, but also in superconducting $La_{2-x}(Ba,Sr)_xCuO_4$ and $YBa_2Cu_3O_{6+x}$. This result suggests the possible existence of *dynamic* stripes, which might be essential to the physics of cuprates and to their superconductivity [***H3**, D. Reznik*].

ITINERANT VIEW OF UNCONVENTIONAL SUPERCONDUCTORS, QUANTUM CRITICALITY, HIDDEN ORDER

In Sr_2RuO_4, a superconducting compound isostructural to $La_{2-x}Sr_xCuO_4$, itinerant magnetic models can capture the main characteristics of the spin excitation spectra. Recent inelastic neutron scattering measurements have therefore focused on a quantitative description of the spin susceptibility, which can then be implemented into spin-exchange models proposed to account for *p*-wave superconductivity in this system (Ph. D. thesis of P. Steffens, Univ. of Cologne).

Unusual spin-triplet collective excitations developing only in the superconducting state of high-T_c cuprates have raised a great deal of interest. Recent inelastic neutron scattering studies of the dispersion of these modes (Ph. D. thesis of S. Pailhès, LLB) and their anisotropy (thesis of V. Hinkov, MPI Stuttgart) suggest that they have mainly quasi-2D character — aside from an energy-dependent 1D anisotropy, and can be quite well described as a triplet spin exciton. This picture implies a homogeneous electronic liquid, in contrast to the alternative (inhomogeneous) stripe picture also proposed to account for the physics of cuprates. Quantitative theoretical calculations carried out by F. Onufrieva and P. Pfeuty using Eliashberg equations, try to precisely estimate the role played by those collective modes in the appearance of unconventional superconductivity. [2]
The phase diagram of superconducting cuprates, plotted as a function of charge density, is asymmetric with respect to electron and hole doping. It has been theoretically argued that this asymmetry could correspond to the existence of two topological quantum critical points (QCPs).[2] Neutron scattering measurements on electron-doped cuprates $(Nd,Ce)_2CuO_4$ indicate that the spin gap closes linearly in applied magnetic fields, without the appearance of in-gap states, at variance with the behavior reported for hole-doped materials [***H2**, E. M. Motoyama*].

From a more general point of view, when the QCP corresponds to the end point of an ordered phase, the strong fluctuations associated with the broken symmetry of the ordered phase could be responsible for anomalous electronic properties. This idea, commonly used in connection with superconducting heavy-fermion systems, has also been proposed to be applicable to high-temperature superconductivity. Recently, polarized neutron experiments (thesis of B. Fauqué, LLB) carried out in the elusive pseudo-gap phase of cuprates, have shown that this phase is actually characterized by long-range magnetic order, which may be associated with an array of circulating currents [***H1**, B. Fauqué*]. Interestingly, this circulating-current phase may disappear close to the doping level where the superconducting temperature is maximum.

When superconductivity develops close to a QCP, the appearance of the associated ordered phase can also turn out to be detrimental to superconductivity. The compound Sr_2RuO_4, is known to be close to a quantum critical point, which can be

approached by Ti substitution (thesis of O. Schuman, Univ. of Cologne). Neutron scattering has been used to study how the magnetic order is stabilized around the impurity, but the observed order does not seem to play the leading role in the superconducting pairing. In the isoelectronic compound $(Sr,Ca)_2RuO_4$, the substitution of Ca for Sr, leads to a tilt and a rotation of the oxygen octahedra, which are accompanied by a re-organization of the electronic structure. Inelastic neutron scattering studies are crucial here because, by tracing changes in the spin excitation spectrum, they can reveal how the evolution of the electronic band structure relates to the appearance of metamagnetism and provide useful insight into the new class of QCP, known as "metamagnetic QCP" or "magnetically tuned QCP", which has recently been suggested for the bilayer compound $Sr_3Ru_2O_7$.

QUADRUPOLAR PHENOMENA IN F-ELECTRON SYSTEMS

Neutron diffraction results on light-rare-earth hexaboride alloys ($Ce_xPr_{1-x}B_6$ and $Ce_xNd_{1-x}B_6$) reflect the effects of competing interactions between atoms carrying different types of quadrupole moments, while shedding light on the complex pattern of commensurate and incommensurate structures occurring in an applied magnetic field. Comparison of the neutron data with synchrotron results obtained in Japan on the same materials gives a clue to separating the dependences of magnetic and quadrupole order parameters [***H6**, J.-M. Mignot*]. This work will be extended to alloys with different compositions, as well as to compounds from the skutterudite family, in which even more exotic (hexadecapole) order parameters have been conjectured.

B - Frustrated magnetism

Geometrically frustrated magnetism is characterized, in a classical approach, by a highly degenerate ground state. It gives rise to unusual phase transitions and exotic spin excitations from a novel ground state, whose study by elastic and inelastic neutron scattering is essential for testing theoretical models.

The simplest example of a frustrated magnet is the Ising triangular antiferromagnet, a good realization of which is provided by $CuFeO_2$ (N. Terada, Tokyo Univ. of Science, with A. Gukasov and D. Petitgrand, LLB). The magnetic excitation spectra have been determined in the low-temperature commensurate phase of this compound, where they were found to consist of three branches with a gap, as well as in the "partially disordered" incommensurate state at intermediate temperatures. One to two per cent aluminum doping in $CuFeFe_{1-x}Al_xO_2$ produces a total of four different new phases depending on temperature. Simultaneously magnetic excitations show a dramatic change with the appearance of a new gapless branch. The next step will be to study the effects of magnetic fields on both magnetic structures and magnetic excitations.
A more involved case of geometric frustration is found in the highly-frustrated 2D Kagome-lattice systems, exemplified by Nd-langasite ($Nd_3Ga_5SiO_{14}$). This compound is a good candidate in the search for a spin-liquid state because no magnetic order is found down to 1.5 K despite the existence of strong antiferromagnetic fluctuations. The broad, slightly dispersive excitation around 1 meV observed by a team from Grenoble [3] in triple-axis experiments is in qualitative agreement with theoretical calculations for a classical Heisenberg antiferromagnet on a Kagome lattice. Future studies will be extended to related systems like $Pr_3Ga_5SiO_{14}$.
"Buckled" Kagome lattices, where a lifting of the ground state degeneracy is expected to take place as a result of the distortion, provide an elegant example of order from subleading interactions in a highly frustrated system. In the staircase-distorted 2D Kagome lattice $Ni_3V_2O_8$, no less than four different ordered magnetic phases (two incommensurate and two commensurate) have been reported to occur below 9 K. Single-crystal experiments have now succeeded in identifying three nearly non-dispersive magnetic excitation modes below 1.5 THz in the lowest commensurate phase (thesis of N. Wilson, Univ. of Warwick).

C - Molecule-based magnetism and photomagnetism

In the field of molecule-based magnetism, classical spin-density studies of the ground state of paramagnetic molecules based on flipping-ratio polarized-neutron measurements are still in high demand. Progress in neutron instrumentation opens unmatched opportunities for studying novel effects in photomagnetism

Recently, experiments have been devoted to an asymmetric end-to-end azido double-bridged Cu(II) dinuclear complex [***C4**, C. Aronica*] and that of an AF bidimensional Mn(II) compound in the paramagnetic phase [***C5**, J. Manson*]. This work has been supplemented by a thorough investigation of the magnetic phase diagram of this compound in an external magnetic field.
A very original application of this same technique is demonstrated in the mapping of spin-redistribution due to quantum entanglement in a pure organic magnet (spin tetramer) [***H7**, A. Zheludev*].
Progress made in photomagnetism encompasses the first successful observation of a photoexcited state by neutron powder diffraction on a FeII spin-crossover system [***C6**, A. Goujon*]. Future evolutions of this experimental approach will strongly depend on its applicability to compounds displaying strong photoabsorption. Different possibilities to overcome this problem are now being tested.

It is generally accepted, on the basis of static susceptibility and XANES absorption results, that the photoinduced and thermally quenched high-spin (HS) states are nearly the same. Therefore, the study of thermally quenched states makes it possible to anticipate the properties of the photoinduced HS state. In the thermally quenched state of the (Co-Fe) Prussian-blue analogue and in (Co^{III},W^{IV}) octacyanotungstate, SQUID magnetization measurements suggest the existence of magnetic order.

Neutron diffraction measurements have been carried out in both phases but no evidence for a magnetic order could be found. On the other hand, recent measurements on $[Fe(ptz)_6](BF_4)_2$ under pressure [4] have evidenced that the ferroelastic transition can be dissociated from the spin transition, with the appearance of a new intermediate distorted high-spin state.

New insight in photoexcitation processes in spin-crossover systems has been gained from single-crystal Laue neutron diffraction measurements performed at the ILL. The results demonstrate a gradual homogeneous photoexcitation of Fe^{II} ions under light irradiation at low temperature, in contrast to the nucleation and growth of high-spin domains (denoted "like-spin"), implying a coexistence between the LS and HS phases [*C7, A. Goujon*]. Further studies of the photo-transformation process and of the subsequent relaxation in a single crystal close to the light-induced instability are now in progress.

Rapid developments can be expected in the next few years as a result of the enhanced data acquisition rates provided by the freshly renovated SUPER-6T2 neutron diffractometer [*Instrumentation –**H1**, A. Gukasov*]. Photoexcitation effects will be observable with greatly improved sensitivity, making it possible to address the conditions of the nucleation and growth process at the initial stage of the separation into like-spin phases. More generally, enhanced data collection speed for very small samples will open up new perspectives for powder and single-crystal diffraction on this instrument.

D - Magnetic surface scattering

The LLB offers a large panel of surface scattering techniques, which users can combine in order to fit their needs. Even more flexible experimental conditions are expected from the implementation of new sample environments.

Studies of magnetic thin films structures have expanded tremendously over the last decade, encompassing an ever-growing variety of materials, from 3*d* metals (Fe, Co, Ni) and oxides (manganites, ferrites) to semiconductors (GaMnAs, ZnO:Co) and rare-earth elements (Dy, Er, etc.). Polarized neutron reflectivity is applied routinely in experiments on PRISM. Small angle scattering is used both in a normal scattering geometry (regular SANS) or at grazing incidence (PAPYRUS). Magnetic diffraction studies can also be performed on films down to 20 nm in thickness, using either unpolarized (3T1, 4F1) or polarized (6T2) neutron beams.

In the last two years, about twelve studies have benefited from such combined measurements. The topics were quite diverse: effects of epitaxial strains, modified or suppressed magnetic order in thin films, magnetization surface effects, magnetic micro-structures and nanostructures, etc. Materials studied include MnAs thin films, in which there is a coexistence of ferromagnetic and paramagnetic phases [***C11**, V. Garcia*], multiferroic materials such as $BiFeO_3$, exhibiting both ferromagnetic and ferroelectric properties (H. Béa, CNRS/Thalès, Palaiseau), ultrashort-period Fe/Co superlattices (M. Bjork and G. Andersson, University of Uppsala), FePt/FePt films mixing in-plane and normal-to-plane materials (W. Szuszkiewicz, Polish Acad. of Sciences), and $[YBCO/LSMO]_n$ superlattices for probing the interaction between magnetic and superconducting materials (G. Beutier, CEA/Grenoble).

The above measurements do not require any special sample preparation, nor extensive measuring times, and can now be performed routinely. On the other hand, inelastic scattering measurements in thin films, whose feasibility was demonstrated previously, [5] remain restricted to very specific samples. In the future, efforts will focus on increasing the versatility of the spectrometers, as well as improving the sample environments provided to users. A new polarizing bender is presently being installed on 4F1 in response to requests for polarized neutron diffraction measurements. For reflectivity and SANS, new technological materials, with Tc much in excess of 300 K, will require high-temperature studies. We therefore plan to implement a new device allowing magnetic fields above 1 T to be applied at temperatures up to 400°C. A dedicated magnet system capable of producing fields of several kilogauss for diffraction experiments would also be desirable.

[1] Co-funded by the CEA and the "Région Basse-Normandie".

[2] Chapter "Theory" in this report

[3] R. Balou, J. Robert, V. Simonet, B. Canals, Laboratoire Louis Néel, CNRS Grenoble, K. Marty, P. Bordet, Laboratoire de Cristallographie, CNRS Grenoble, with D. Petitgrand, LLB.

[4] M.-H. Lemée-Cailleau, C. Ecolivet, B. Ouladdiaf, F. Moussa, J. Jeftic, J. F. Létard, International Conference on Magnetism ICM'2006, J. Magn. Magn. Mater., in press.

[5] LLB Scientific Report 2003-2004.

SUPERCONDUCTIVITY AND MAGNESTISM

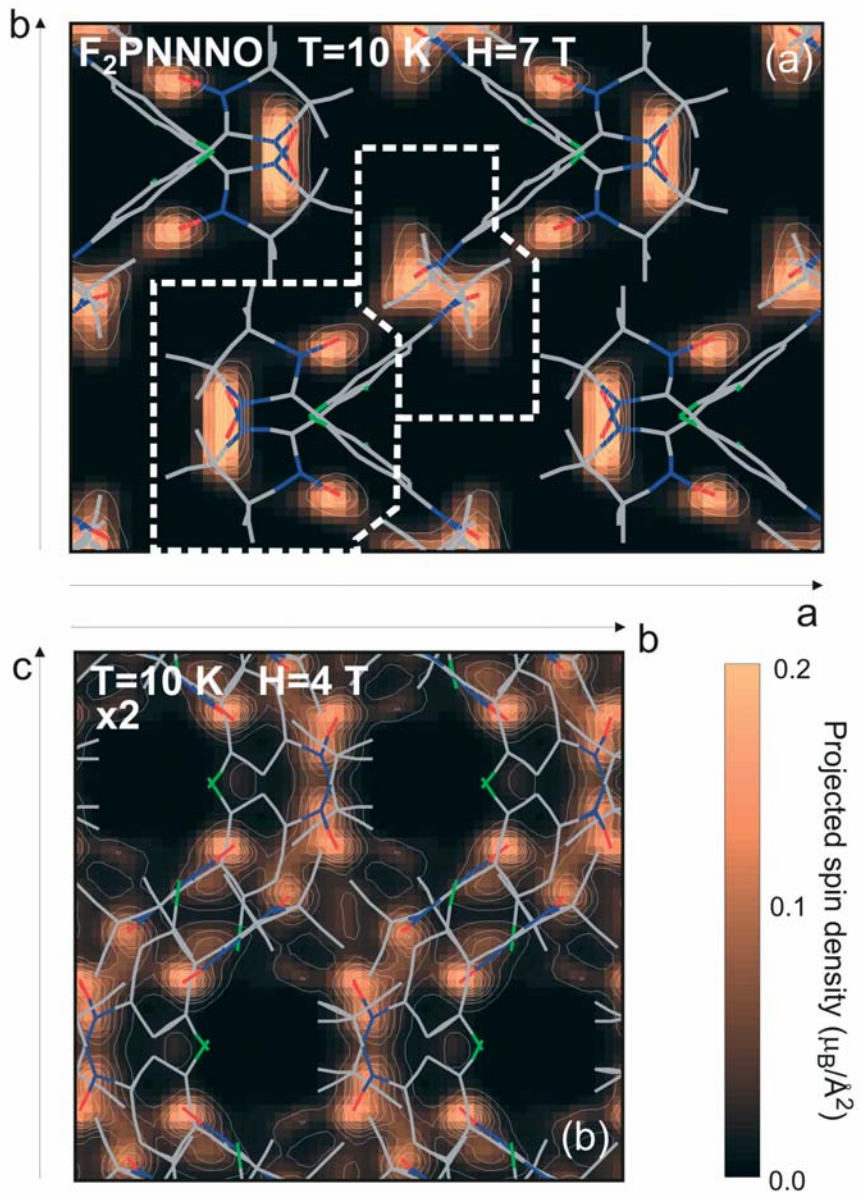

SUPERCONDUCTIVITY AND MAGNESTISM

H1. **Magnetic order in the pseudogap phase of high-T_c superconductors**
B. Fauqué, Y. Sidis, V. Hinkov, S. Pailhès, C.T. Lin, X. Chaud, Ph. Bourges

H2. **Spin-gap Closing under magnetic field in the electron doped high-T_c superconductor**
E.M. Motoyama, D. Petitgrand, M. Greven

H3. **Bond-stretching phonon anomaly reflecting dynamic charge inhomogeneity in copper-oxide superconductors**
D. Reznik, L. Pintschovius, M. Ito, S. Iikubo, M. Sato, H. Goka, M. Fujita, K. Yamada, G. D. Gu, J.M. Tranquada

H4. **A 2D stripe superstructure revealed by spin waves in cubic ferromagnetic $La_{1-x}Sr_xMnO_3$ (x = 0.125 and x = 0.15)**
S. Petit, M. Hennion, F. Moussa, P. Reutler, A. Revcolevskii, Y. M. Mukovskii

H5. **Spin-wave dispersion in orbitally ordered $La_{0.5}Sr_{1.5}MnO_4$**
D. Senff, F. Krüger, S. Scheidl, M. Benomar, Y. Sidis, F. Demmel, M. Braden

H6. **Competing order parameters in light-rare-earth hexaborides**
J.-M. Mignot, G. André, M. Sera, and F. Iga

H7. **Spin redistribution by entanglement in an organic magnet**
A. Zheludev, V. O. Garlea, S. Nishihara, Y. Hosokoshi, A. Cousson, A. Gukasov, K. Inoue

[*C1.* **S. P. Bayrakci**]
Magnetic Ordering and SpinWaves in $Na_{0.82}CoO_2$

[*C2.* **O. Mentré**]
Spin gap in the one-dimensional *S* = 1/2 spin-ladder compound $Bi_2Cu(P1-_xV_x)O_6$

[*C3.* **S.M. Yusuf**]
Two- and three-dimensional magnetic ordering in the bilayer manganite $Ca_{2.5}Sr_{0.5}GaMn_2O_8$

[*C4.* **C. Aronica**]
Ferromagnetic Interaction in an Asymmetric End-to-End Azido Double-Bridged Copper(II) Dinuclear Complex

[*C5.* **J. Manson**]
Neutron diffraction study of a molecule-based 2-dimensional magnetic compound $Mn(dca)^2(pym)(H_2O)$: spin density and magnetic phase diagram.

[*C.6.* **A. Goujon**]
Photoswitchable molecular compounds studied by neutron powder diffraction

[*C7.* **A. Goujon**]
Neutron Laue diffraction on the spin crossover crystal $[Fe(ptz)_6](BF_4)_2$ showing continuous photo-induced transformation

[*C8.* **A. Tamion**]
Magnetization depth profile of (Fe/Dy) multilayers

[*C9.* **M. Delalande**]
Polarized SANS studies of FePt Magnetic Nanoparticles.

[*C10.* **G. Viau**]
Small Angle polarised neutrons studies of dispersed magnetic Co-Ni nanowires

[*C11.* **V. Garcia**]
Magneto-structural phase transition in MnAs epilayers grown on GaAs(111)B substrates

H1. MAGNETIC ORDER IN THE PSEUDOGAP PHASE OF HIGH-TC SUPERCONDUCTORS

B. FAUQUÉ[1], Y. SIDIS[1], V. HINKOV[2], S. PAILHÈS[1,3], C.T. LIN[2], X. CHAUD[4], PH. BOURGES[1]

[1] Laboratoire Léon Brillouin, CEA-CNRS, CEA/Saclay, 91191 Gif sur Yvette, France
[2] MPI für Festkörperforschung, Heisenbergstr. 1, 70569 Stuttgart, Germany
[3] LNS, ETH Zurich and Paul Scherrer Institute, CH–5232 Villigen PSI, Switzerland
[4] CRETA/CNRS, 25 Avenue des Martyrs, BP 166, 38042 Grenoble cedex 9, France.

In the optimally doped and underdoped regimes, high-T_c copper oxide superconductors (SC) exhibit a pseudogap state with anomalous magnetic, transport, thermo-dynamic, and optical properties below a temperature, T^*, which is large in comparison to the super-conducting transition temperature, T_c. The origin of the pseudogap is a challenging issue as it might eventually lead to identify the superconducting mechanism. Two major classes of theoretical models attempt to describe the pseudogap state: in the first case, it represents a precursor of the superconducting *d*-wave gap with preformed pairs below T^*, which would acquire phase coherence below T_c. In a second approach, the pseudogap is associated either with an ordered or with a disordered phase competing with the SC state. The order parameter associated with these competing phases may involve charge- and spin- density waves, or charge currents flowing around the CuO_2 square lattice, such as D-charge density wave (DDW) or orbital circulating currents (CC) as proposed by C. M. Varma [1].

Most of the above phases break the translation symmetry of the lattice (TSL). Therefore, they may induce charge, nuclear or magnetic superstructures that can be probed by neutron or x-ray diffraction techniques. In contrast, the novel CC phases preserve the TSL as they correspond to 4 or 2 current loops per unit cell [1]. The charge currents could be identified by virtue of the pattern of ordered orbital magnetic moments pointing perpendicularly to the CuO_2 planes (*i.e.*, along c^*). These orbital magnetic moments should be detectable by neutron diffraction. Although the TSL is preserved, the magnetic signature of the CC phase does not reduce to ferromagnetism: the loops are staggered within each unit cell which corresponds to a zero magnetic propagation wavevector, $\boldsymbol{Q} = 0$, but with no net magnetization. In neutron diffraction, the magnetic intensity is superimposed on the nuclear Bragg peak, meaning that these experiments are very delicate as the magnetic intensity, proportional to the squared magnetic moment M^2, is expected to be very small as compared to the nuclear Bragg intensity. In order to detect this hidden magnetic response, polarized neutron experiments, which allow us to separate magnetic and nuclear cross sections, are therefore required.

Motivated by this theoretical work, we have studied the possibility of a magnetic order associated to these circulating current phases. Polarized neutron measurements were performed on the triple-axis spectrometer 4F1, using full polarization analysis. We have reported the first successful observation of a magnetic order in the pseudogap state of the cuprate $YBa_2Cu_3O_{6+x}$ [2]. Since this type of phase does not break the translational symmetry, the magnetic contribution occurs only on top of the nuclear Bragg peaks, and we thus measured the magnetic signal on the weakest Bragg peak: the (011) reflection provides the best compromise between the magnetic scattering amplitude and the leakage of the Bragg scattering into the spin-flip channel. For the neutron polarization $\boldsymbol{P}$ // $\boldsymbol{Q}$, where one expects the magnetic scattering to be strongest, the spin-flip (SF) intensity increases notably at low temperature, in contrast of the non-spin-flip (NSF) intensity which is essentially flat (Fig. 1). To assess the reproducibility of our observation, we have studied a large variety of samples from the underdoped part of the phase diagram of the high-T_c compound family $YBa_2Cu_3O_{6+x}$ with T_c ranging from to 54 K in underdoped samples to 75 K in an overdoped sample.

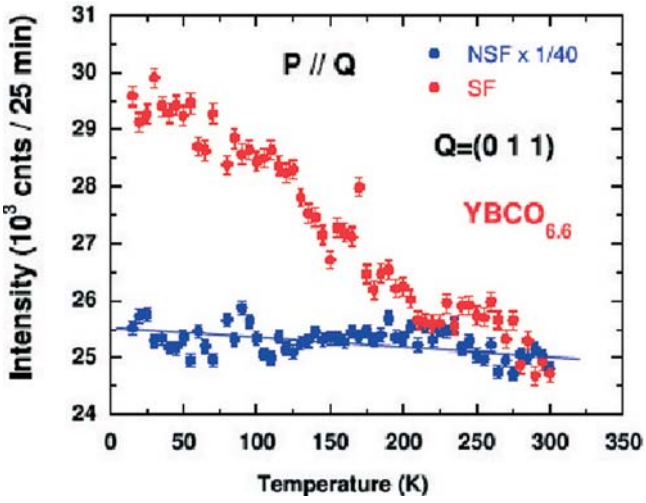

Figure 1. Raw polarized-neutron intensity : the full red points show the spin-flip (SF) scattering and the blue ones the non-spin-flip (NSF) scattering. A signal occurs below ⊕220 K only in the SF channel.

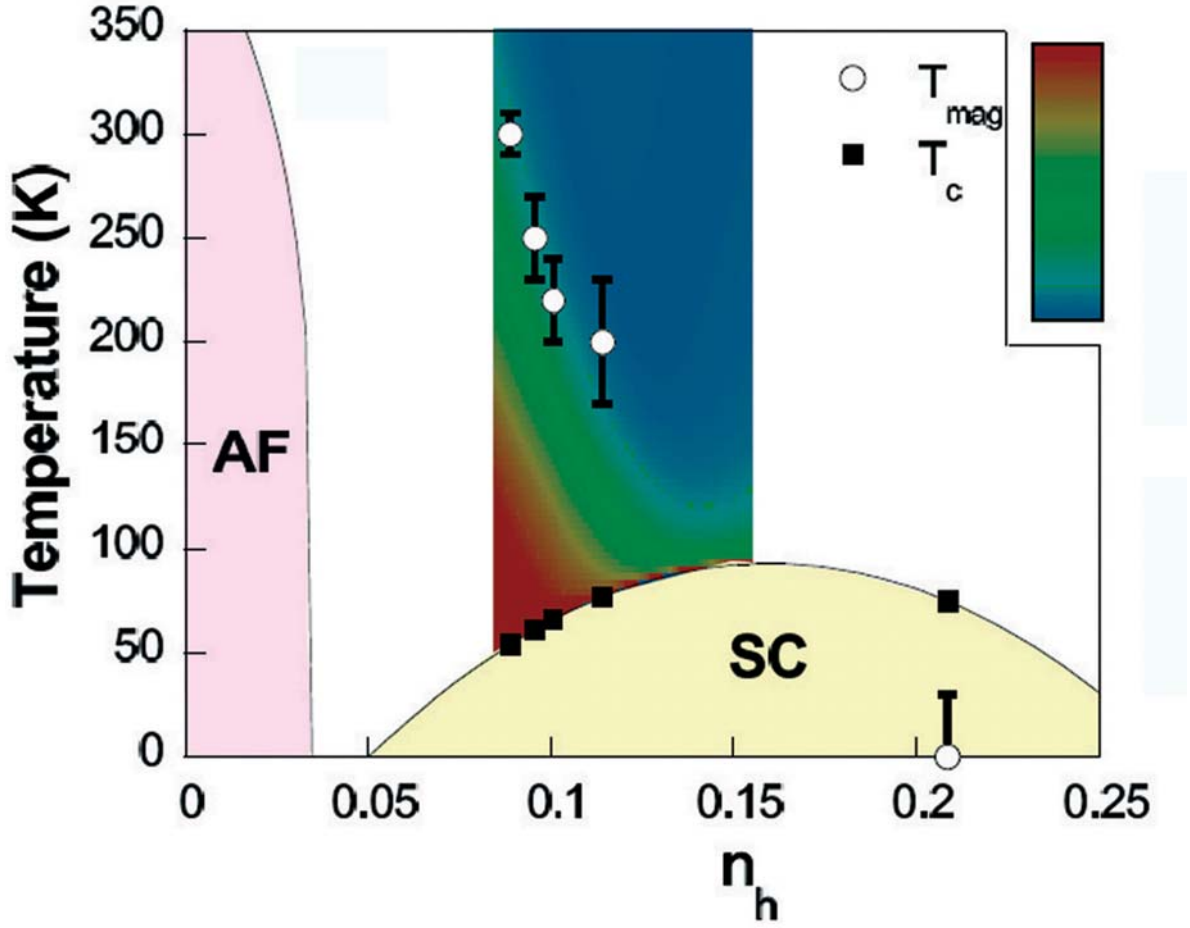

Figure 2. High-T_c phase diagram as a function of the hole doping. The coloured area (blue=0) shows the pseudogap phase as measured by resistivity. T_{mag} is the temperature where the magnetic order occurs.

The results demonstrate the appearance of a magnetic scattering in the SF channel below a temperature T_{mag}, that matches quite well the pseudogap temperature T^* as defined by the resistivity measurement (Fig. 2). The magnitude of the observed signal changes with the neutron polarization as is expected for a magnetic intensity. This definitively rules out any experimental artefact.

The typical cross section of the magnetic order is $\oplus 10^{-4}$ of the strongest Bragg peaks. This explains why such a magnetic order was not detected before using unpolarized neutron diffraction. Using the observed magnetic cross section and assuming a weakly momentum-dependent form factor, one can deduce a typical magnitude for the ordered magnetic moment of about 0.05 to 0.1 μ_B, with a moment decreasing with increasing doping. This is about the magnitude expected from current loops in the CC phase. However, such an orbital moment is expected to lie perpendicular to the CuO_2 planes, whereas, in our case, the moments are not purely along the c* axis. Combining the data for all measured polarizations in the different samples, one can estimate the mean angle between the direction of the moments (assumed to be collinear) and the c^* axis to be _ = 45° ± 20°, valid for all samples. In summary, we have reported the first signature of an unusual magnetic order in several $YBa_2Cu_3O_{6+x}$ samples matching the pseudogap behaviour in underdoped high-Tc cuprates [2]. Such an observation points towards the existence of a hidden order parameter for the pseudogap phase in high-Tc superconductors. Importantly, our experiment reveals a 3D long-range order which does not break the translational symmetry of the lattice and, therefore, implies a decoration of the unit cell with staggered spin or orbital moments. The symmetry of the observed order corresponds to that expected for orbital moments associated with a circulating current state [1].

[1] C.M. Varma, Phys. Rev. B 55, 14554 (1997); *ibid.* **73**, 155113 (2006).
[2] B. Fauqué et al, Phys. Rev. Lett. **96**, 197001 (2006).

H2. SPIN-GAP CLOSING UNDER MAGNETIC FIELD IN THE ELECTRON-DOPED HIGH-TC SUPERCONDUCTOR: $Nd_{1.85}Ce_{0.15}CuO_4$

E.M. MOTOYAMA[1], D. PETITGRAND[2], M. GREVEN[1]

[1] Department of Physics, Stanford University, Stanford, California 94305, USA
[2] Laboratoire Léon Brillouin (CEA-CNRS), CEA/Saclay, 91191 Gif sur Yvette Cedex

Understanding the nature of superconductivity in high-T_c superconductors requires the characterization of the various phases (antiferromagnetic insulating, spin-density wave, charge-density wave…) that may compete with the superconducting state.
Up to now, this has been achieved mainly by studying the properties of these compounds upon varying external parameters such as the carrier concentration or the temperature. However, the effect of a strong magnetic field has been much less studied. As a consequence, the nature of the field-induced ground state is still an open question.

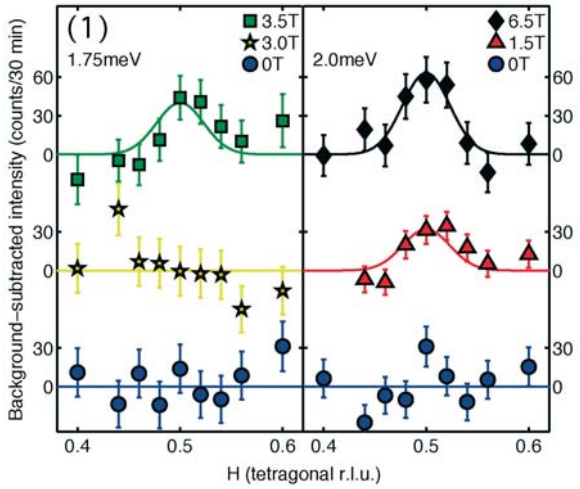

Figure 1. Transverse scans (h 1-h 0) through the AF zone center (1/2, 1/2, 0) at an energy transfer of ε = 1.75 meV (left) and ε = 2.0 meV (right). Before each scan, the sample was field-cooled from above T_c to T = 1.8 K. Typical counting time is 30 min. per point.

In this study, we use inelastic neutron scattering to determine the magnetic-field effect on the superconducting spin-gap of $Nd_{2-x}Ce_xCuO_4$, the prototype of electron-doped high-T_c superconductors. A detailed report of the results was published in Ref. [1]. The dynamic susceptibility $\chi''(\boldsymbol{q}_0,\varepsilon)$ near the antiferromagnetic (AF) point $\boldsymbol{q}_0$ = (1/2, 1/2, 0) has been measured as a function of energy for different magnetic fields using the same method as used in our previous zero-field study [2].
In Fig.1, showing a typical q scan at constant energy for different fields, one sees how an applied magnetic field can cause the signal, which was initially suppressed by the spin-gap opening, to reappear. Before each scan, the sample was first heated above T_c and then cooled down in the new field back to T = 1.8 K; this procedure was followed in order to ensure a macroscopically uniform internal field. At an energy transfer of ε = 1.75 meV [Fig. 1(*a*)], the magnetic excitations are completely suppressed up to H = 3 T, and reappear at 3.5 T. A similar behavior is seen at the slightly higher energy transfer of ε = 2.0 meV [Fig. 1(b)]. In this case, the peak is seen to reappear at a lower field of H = 1.5 T

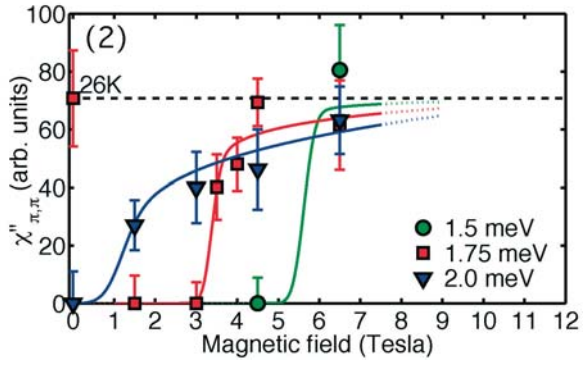

Figure 2. Dynamic susceptibility $\chi''(\boldsymbol{q}_0,\varepsilon)$ at $\boldsymbol{q}_0$ = (1/2, 1/2, 0) as a function of field at several energies. All data are taken at T = 1.8 K except the zero-field point at T = 26 K.

Figs. 2 to 4 summarize the experimental results obtained on the triple-axis spectrometer 4F2 at LLB.
For hole-doped materials, the upper critical field at which superconductivity is completely destroyed is ~50 T or larger [3], prohibitively large for neutron scattering experiments. For the electron-doped materials, on the other hand, H_{c2} is relatively lower (~10 T) [3], which has allowed us to observe a field effect on the superconducting magnetic gap in $Nd_{2-x}Ce_xCuO_4$ up to high values of the relative magnetic-field strength.
Fig. 2 shows the evolution of the magnetic signal with magnetic field for energies within the zero field gap. The signal remains zero up to a threshold field which depends on energy. Then the signal increases with field, which is a first indication that the gap decreases. The horizontal dashed line represents the signal measured above T_c (T = 26 K) showing that the dynamical susceptibility at high H and low T is essentially the same as above T_c in zero field.

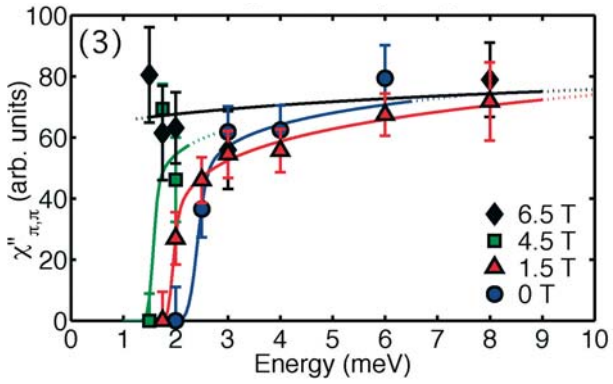

Figure 3. Field dependence of the magnetic excitation spectrum $\chi''(\boldsymbol{q}_0,\varepsilon)$ as a function of energy at T = 1.8 K. Curves are guides to the eye.

Fig. 3 shows the dynamical susceptibility $\chi''(\boldsymbol{q}_0,\varepsilon)$ for several fields up to 6.5 T. The zero-field gap energy in our sample is 2.5 meV, slightly smaller than in a previous work [2], in accordance with our somewhat lower T_c. It decreases down to 1.5 meV at 5 T. At H = 6.5 T, we have not been able to measure the gap because of the dominating magnetic excitations of Nd at low energies. These results can be interpreted as a rigid down shift of the gap profile with field.

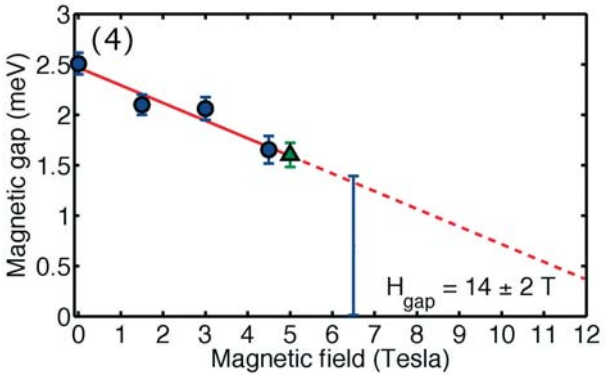

Figure 4. Evolution of the magnetic gap (half-maximum energy) as a function of field. The dependence is linear and extrapolates to zero at H_{gap} ~14.2 T. The vertical bar reflects the fact that the gap energy is less than 1.5 meV.

Our results do not show any field-induced excitation in the gap as reported for the $La_{2-x}Sr_xCuO_4$ compound [4-6].
In Fig. 4, the gap energy is plotted as a function of field. The magnetic gap decreases linearly with field, and collapses completely at an extrapolated value of H_{gap} ~14.2 T, consistent with an upper critical field of H_{c2} ~10–12 T [3].
The gapped spectrum of $Nd_{2-x}Ce_xCuO4$ undergoes a rigid shift towards lower energies as the magnetic field is increased, which is in strong contrast to the formation of in-gap states in optimally doped and slightly overdoped $La_{2-x}Sr_xCuO_4$ [4-6]. Because measurements below 1.5 meV were not possible, it is natural to ask whether the formation of some in-gap states in $Nd_{2-x}Ce_xCuO_4$ could be hidden below this energy. However, we emphasize that the signal strength at 1.5 meV remains zero up to 4.5 T. Since our energy resolution is 1.3 meV (full width at half maximum), the experiment is sensitive to any in-gap intensity down to very low energies.
The results point to a picture in which the non-superconducting ground state at fields above H_{c2} does not possess magnetic order, but is a paramagnet with AF fluctuations. The first piece of evidence is that, in $Nd_{1:85}Ce_{0:15}CuO_4$, applying a magnetic field and increasing temperature have similar effects, and the gap does not appear to close until superconductivity is completely suppressed [7]. Moreover, the signal strength seen at high magnetic fields equals that in the normal state just above T_c. All of this indicates that the non-superconducting ground state beyond H_{c2} resembles the paramagnetic normal state above T_c.
The absence of magnetic-field-induced in-gap states in $Nd_{1:85}Ce_{0:15}CuO_4$ and the likely absence of field-induced magnetic order imply an important difference between the electron-doped and hole-doped cuprates; the competing spin- (and charge-) density wave order (often referred to as "stripes") observed in hole-doped superconductors, especially in materials derived from the high-T_c parent compound La_2CuO_4, hinders an unobstructed study of the AF-correlated superconductor due to the presence of a nearby quantum critical point. This complication appears to be avoided by the electron-doped materials, which possess the additional experimental advantage of a relatively low upper critical field.

[1] E.M. Motoyama, P.K. Mang, D. Petitgrand, G. Yu, O.P. Vajk, I.M. Vishik and M. Greven Phys. Rev. Lett., **96**, 137002 (2006)
[2] D. Petitgrand, K. Yamada, M. Fujita, and T. Uefuji, Physica C **408–410**, 778 (2004).
[3] Y. Wang et al., Science **299**, 86 (2003).
[4] B. Lake et al., Science **291**, 1759 (2001).
[5] J. M. Tranquada et al., Phys. Rev. B **69**, 174507 (2004).
[6] R. Gilardi et al., Europhys. Lett. **66**, 840 (2004).
[7] K. Yamada et al., Phys. Rev. Lett. **90**, 137004 (2003).

H3. BOND-STRETCHING PHONON ANOMALY REFLECTING DYNAMIC CHARGE INHOMOGENEITY IN COPPEROXIDE SUPERCONDUCTORS

D. REZNIK[1,2], L. PINTSCHOVIUS[1], M. ITO[3], S. IIKUBO[3], M. SATO[3], H. GOKA[4*], M. FUJITA[4], K. YAMADA[4], G. D. GU[5], AND J.M. TRANQUADA[5]

[1] Forschungszentrum Karlsruhe, Institut für Festkörperphysik, P.O.B. 3640, D-76021 Karlsruhe, Germany
[2] Laboratoire Léon Brillouin, CE Saclay, F-91191 Gif-sur-Yvette Cedex, France
[3] Department of Physics, Division of Materials Science, Nagoya University, Furo-cho, Chikusa-ku, Nagoya 464-8602, Japan
[4] Institute for Material Research, Tohoku University, Katahira, Aoba-ku, Sendai, 980-8577, Japan.
[5] Condensed Matter Physics and Materials Science Department, Brookhaven National Laboratory, Upton, New York 11973-5000, USA

While many believe that antiferromag-netism is important for the high-temperature superconduc-tivity, there has been resurgent interest in the role of electron-lattice coupling. The Karlsruhe group, in collaboration with others, has been investigating electron-phonon coupling due to charge inhomoge-neities in copper oxide superconductors. This work focused on detailed measurements of optic oxygen modes believed to couple most strongly to dynamic charge inhomogeneity. The 1T spectrometer is ideally suited for such a study, as its performance is optimized for the high energies of these phonons. A collaboration with the theory group in Karlsruhe (K-P. Bohnen and R. Heid), made it possible to compare experimental results to predictions of band theory and thus separate the conventional Fermi-liquid physics from still poorly understood correlation effects.

Band theory works remarkably well for predicting electron-phonon effects in the recently studied conventional superconductors MgB_2 and YNi_2B_2C. They have a very strong electron-lattice coupling involving a particular phonon that was predicted by band theory and confirmed quantitatively by experiment. Our inelastic neutron scattering meas-ure-ments showed that there is a similarly strong anomaly in the Cu-O bond-stretching phonon in cuprate superconductors La^2-$_x$Sr$_x$CuO$_4$ (x = 0.07, 0.15) and in $YBa_2Cu_3O_{6+x}$ (x = 0.6, 0.95); however, this behavior is completely absent in band theory calculations. Instead, the anomaly is strongest in $La_{1.875}Ba_{0.125}CuO_4$ and $La_{1.48}Nd_{0.4}Sr_{0.12}CuO_4$, compounds that exhibit spatially modulated long-range charge and magnetic order, often called stripe order. It occurs at a wave vector corresponding to the charge order.

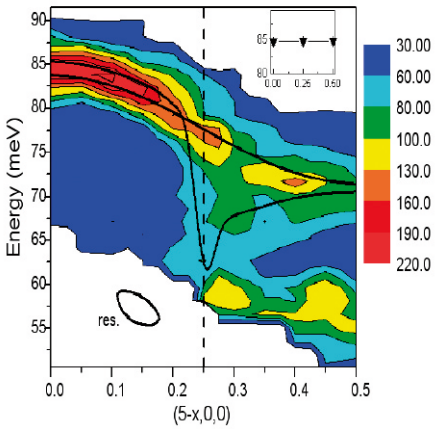

Figure 1. Color-coded contour plot of the intensities observed on $La_{1.875}Ba_{0.125}CuO_4$ at T = 10 K. The intensities above and below 60 meV are associated with plane-polarized Cu-O bond-stretching vibrations and bond-bending vibrations, respectively. Black lines are dispersion curves evaluated from two-peak fits to the data. The white area at the lower left corner of the diagram was not accessible in this experiment. The ellipse illustrates the instrumental resolution. The inset shows the dispersion in the [110]-direction. The dashed line represents the charge–ordering wavevector.

Stripe order is known to result from strong electron-electron correlations due to Mott physics. While the static stripe compounds are not superconductors, many believe that dynamic stripes play a crucial role in the physics of the cuprates and, possibly, in the mechanism of high T_c superconductivity. Existence of dynamic stripes is still controversial. Observation of a very similar anomaly in compounds with and without static stripes suggests that they may be present throughout the doping range associated with superconductivity (the anomaly is absent in undoped and overdoped non-superconductors).

More importantly, the phonon measurements conclusively demonstrated that a strong charge fluctuation, not predicted by band theory, is present in copper oxide superconductors and that it strongly couples to phonons. It follows that electron-phonon coupling may be important to understanding the superconductivity although its contribution to the mechanism is likely indirect.

[1] D. Reznik, L. Pintschovius, M. Ito, S. Iikubo, M. Sato, H. Goka, M. Fujita, K. Yamada, G.D. Gu, and J.M. Tranquada, Nature 440, 1170 (2006).

[2] L. Pintschovius, D. Reznik, and K. Yamada, to appear in Phys. Rev. B

H4. A 2D STRIPE SUPERSTRUCTURE REVEALED BY SPIN WAVES IN CUBIC FERROMAGNETIC $La_{1-x}Sr_xMnO_3$ (x = 0.125 and x = 0.15)

S. PETIT[1], M. HENNION[1], F. MOUSSA[1], P. REUTLER[2], A. REVCOLEVSKII[2] AND Y. M. MUKOVSKII[3]

[1] Laboratoire Léon Brillouin CEA-CNRS, CE Saclay, 91191, Gif-sur-Yvette Cedex, France
[2] Laboratoire de Physico-Chimie des Solides, Université Paris-Sud, 91405 Orsay Cedex, France
[3] Moscow State Steel and Alloys Institute, Moscow 119991, Russia

Manganites La(Ca,Sr)MnO_3 belong to a large class of compounds in which the strong correlations among electrons are suspected to be responsible for nanoscale charge segregation effects. In these oxides, the hole concentration can be tuned by substituting Ca or Sr on the La-sites. At zero doping, the spins of Mn form ferromagnetic (***a***,***b***) planes stacked antiferro-magnetically along the ***c*** axis. Upon doping, a new ferromagnetic coupling resulting from the double-exchange mechanism becomes effective and stabilizes a ferromagnetic, metallic state beyond $x \sim 0.2$. However, the way this compound evolves towards the new phase is very peculiar, emphasizing the role of charge segregation. We have shown previously [1] that at low doping, *hole-rich* platelets embedded in a hole-poor matrix are formed within the (***a***,***b***) planes. Neutron scattering experiments enabled us to determine their size (~16 Å) and their liquid-like distribution. As x increases, these platelets grow and percolate for $x = 0.12$, while the antiferromagnetic coupling along ***c*** concomitantly becomes zero. Beyond this concentration, inelastic neutron scattering experiments show that the magnetic excitation spectrum consists of a dispersed branch at small q, and several discrete modes at larger q. The former indicates long-range ferromagnetically coupled spins, while the latter are attributed to standing spin waves within small ferromagnetic domains. Moreover, recent experiments carried out as a function of temperature in $La_{7/8}Sr_{1/8}MnO_3$ [2] and in $La_{0.85}Sr_{0.15}MnO_3$ [3] revealed the occurrence of a gap at $q = 1/8$, indicating a new periodicity of 4 lattice spacings within the (***a***,***b***) planes (Fig. 1*a*). In connection with the low doping regime, we propose an interpretation in terms of reverse charge segregation. In this picture, *hole-poor* 4 x 4 ferromagnetic clusters tend to form on manganese sites within the (***a***,***b***) planes. Those clusters are weakly coupled across hole-rich boundaries located on oxygen sites (Fig. 2), leading to a superstructure of orthogonal stripes. This picture is quite well supported by spin-wave calculations [3] (Fig. 1*b*). This is, to our knowledge, the first observation 0 of stripes in a ferromagnetic state.

[1] M. Hennion, F. Moussa *et al.*, Phys. Rev. Lett. **81**, 1957 (1998); *ibid.* **94**, 57006 (2005).

[2] M. Hennion, F. Moussa *et al.* Phys. Rev. B **73**, 104453 (2006).

[3] S. Petit, M. Hennion, F. Moussa *et al.*, Workshop on Self-organized Strongly Correlated Electron Systems, Seillac (France) May 29-31, 2006.

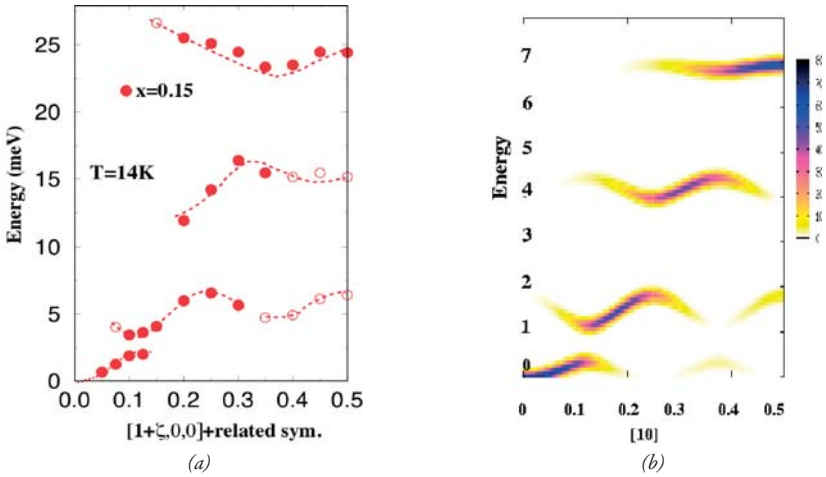

(a) *(b)*

Figure 1

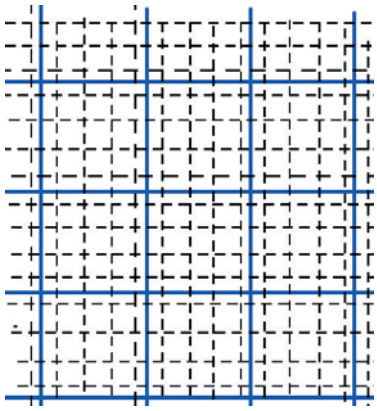

Figure 2

H5. SPIN-WAVE DISPERSION IN ORBITALLY ORDERED $La_{0.5}Sr_{1.5}MnO_4$

D. SENFF[1], F. KRÜGER[2,3], S. SCHEIDL[2], M. BENOMAR[1], Y. SIDIS[4], F. DEMMEL[5], AND M. BRADEN[1],

[1] II. Physikalisches Institut, Universität zu Köln, Zülpicher Str. 77, D-50937 Köln, Germany
[2] Institut für Theoretische Physik, Universität zu Köln, Zülpicher Str. 77, D-50937 Köln, Germany
[3] Instituut-Lorentz, Universiteit Leiden, P.O. Box 9506, 2300 RA Leiden, The Netherlands
[4] Laboratoire Léon Brillouin, CEA-CNRS, F-91191 Gif sur Yvette Cedex, France
[5] Institut Laue Langevin, BP 156, 38042 Grenoble Cedex 9, France

The colossal magneto-resistivity in manganites is only partially explained by the Zener double-exchange mechanism; the larger part of it appears to arise from the competition of two states: the metallic ferromag-netically ordered state on the one side and the insulating one with a cooperative ordering of charges, orbitals and spins (COS) on the other side [1, 2]. The insulator-to-metal transition consists in switching from a phase with long or short-range COS correlations into the metallic state where spins are aligned either by an external field or by spontaneous magnetic order. The combined COS ordering has first been studied in the pioneer work by Wollan and Koehler [3] and by Goodenough [4] proposing the so-called CE-type arrangement, which is illustrated in Fig. 1(*a*). For half doping, i.e. equal amounts of Mn^{3+} and Mn^{4+}, there is a checkerboard arrangement of different charges. In addition the e_g orbitals at the Mn^{3+} sites form zigzag chains. The CE-type charge and orbital arrangement will yield a ferromagnetic interaction in the zigzag chains and an [antiferromagnetic] interaction in-between.

The magnetic excitations in the ferromagnetic metallic manganites have been studied for many different compositions (for a recent summary see Ref. [5]). In view of the large amount of data on the ferromagnetic phases, it may be surprising that there is still no detailed study of magnetic excitations in the antiferromagnetic COS states. Besides the intrinsic complexity of the CE-type magnetic ordering, such a study is severely hampered by the twinning of the manganite crystals in the perovskite phases. We, therefore, have chosen the layered material $La_{0.5}Sr_{1.5}MnO_4$ to study the magnon dispersion in the COS state (Fig. 1).

We were able to separate the magnon branches parallel and perpendicular to the zigzag-chains, as only one twin orientation contributes to a given quarter-indexed magnetic superstructure reflection. When going from the *antiferromagnetic* zone center (0.75,-0.75,0) along the [1,1,0] direction one determines the spin-wave dispersion parallel to the zigzag chains (Fig. 2, right) and, when going along the [1-10] direction, one measures the dispersion perpendicular to the chains. This behavior is corroborated by the structure factor calculations presented in Fig. 2 as discussed below. The raw-data scans unambiguously demonstrate that

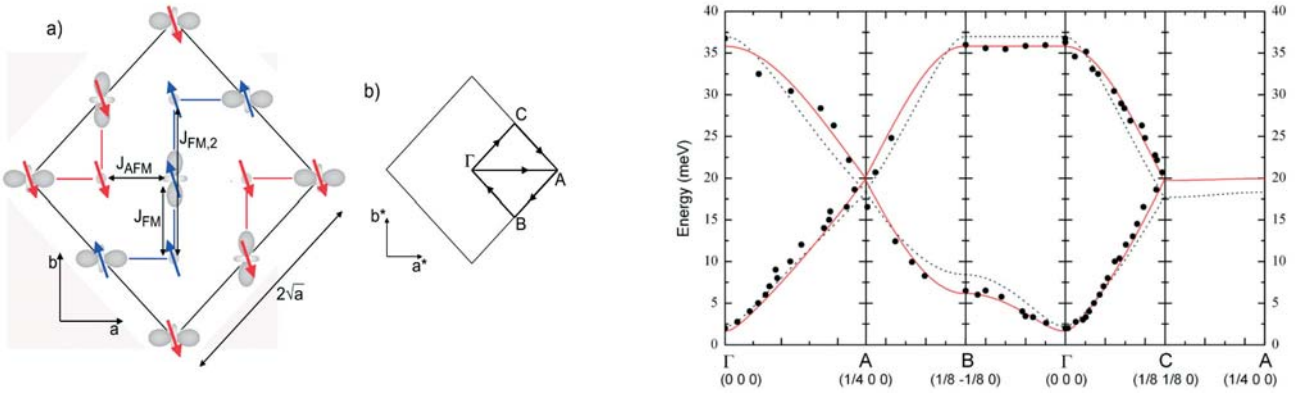

Figure 1. (a) Schematic representation of the CE-type ordering in the (*a,b*) plane of half-doped manganites with three magnetic interactions parameters. Notice that the FM zigzag chains run along the [110] direction. (*b*) Sketch of the magnetic Brillouin zone, displaying the high-symmetry points Γ = (0, 0, 0), *A* = (1/4, 0, 0), *B* = (1/8, -1/8, 0), *C* = (1/8, 1/8, 0) and the path of the calculated dispersion. (*c*) Dispersion of the magnetic excitations in $La_{0.5}Sr_{1.5}MnO_4$ in a direction parallel to [100] (Γ–*A*), perpendicular to the chains (Γ–*B*) and parallel to the chains (Γ–*C*). The solid and broken lines give the spin-wave dispersion calculated with a two parameter set.

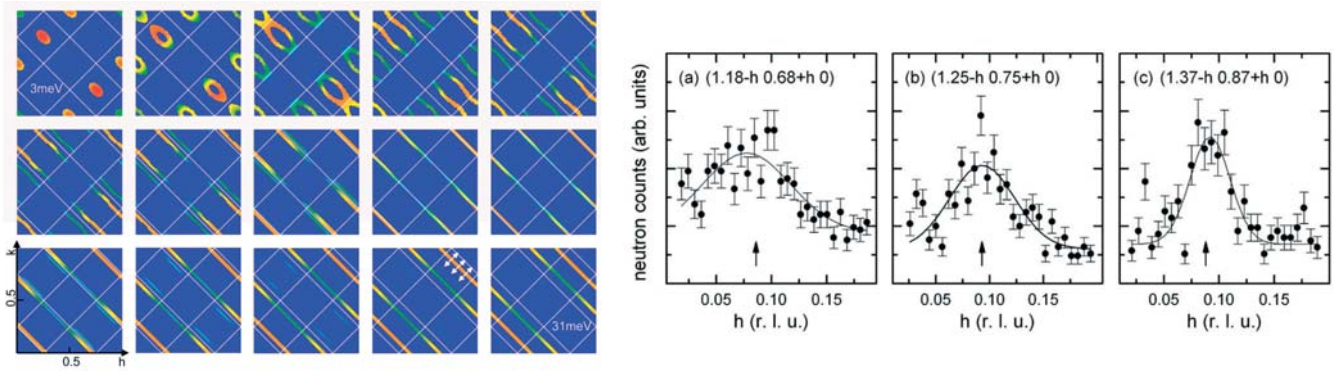

Figure 2. (left panel): Constant energy cuts through the calculated spin-wave structure factor with constant energy resolution of 2 meV within each plot, and with energy steps of 2 meV between adjacent plots, showing the dispersion and scattering distribution of the lowest magnon bands. (right panel): Constant energy scans along the direction indicated by arrows in the 29 meV cut (above) to experimentally verify the one-dimensional character of the high-energy magnetic scattering. The arrows indicate the expected positions of the magnon.

the dispersion along the zigzag chains is much steeper than perpendicular to them. The magnetic structure has to be considered as a weak antiferromagnetic coupling of strongly coupled ferromagnetic zigzag chains. The obtained magnon dispersion is presented in Fig. 1(*c*). The branch propagating along the chains (Γ–*C* path), is much steeper than the branch propagating perpendicular to it, (Γ–*B* path). At the magnetic zone boundaries *C* and *B* we find magnon energies of 19meV and 6.5 meV, respectively. At the C point where *q* is parallel to the chains, the end-point of the acoustic branch coincides with that of the lowest optic branch, whereas there is a large gap between these branches along the Γ–*B* path. The magnon branch along the [100] direction (Γ–A path, at 45° with respect to the chains), exhibits an intermediate dispersion.

The spin-wave dispersion has been calculated using the Holstein-Primakoff transformation with a simple spin-only Hamiltonian illustrated in Fig. 1(*a*). The Mn^{3+} and Mn^{4+} spins were fixed to the values $S = 2$ and $S = 1.5$, respectively. Taking into account only the two nearest-neighbor Mn^{3+}–Mn^{4+} spin interactions for pairs within and in-between the zigzag chains, J_{FM} and J_{AFM}, one obtains a good description of the measured dispersion denoted by broken lines in Fig. 1(*c*). However, there remain significant discrepancies: it is impossible to simultaneously describe the large initial slope of the spin-wave dispersion along the chains and the relatively lower zone-boundary frequencies. This behavior implies the relevance of an additional longer-distance interaction parameter acting along the ferromagnetic chains. Indeed, a fully satisfactory description is obtained by including a ferromagnetic interaction for Mn^{4+}–Mn^{4+} spin pairs connected through a Mn^{3+} site within a zigzag chain. Fig. 2 (left) presents the calculated magnon scattering intensities in the form of constant energy cuts. One can see how the anisotropic spin-wave cones develop around the magnetic Bragg peaks with finite structure factor. At intermediate energies those magnetic Brillouin zones in which there is no elastic scattering also contribute. Fig. 2 further illustrates that, well above the maximum of the acoustic magnon perpendicular to the zigzag chains, the system looks like a magnetically one-dimensional system as the magnons disperse only along the zigzag chains. The one-dimensional character was verified by special constant-energy scans (Fig. 2). The dominant ferromagnetic coupling is further seen in experiments upon heating across the charge and orbital ordering.

The strong ferromagnetic interaction in the zigzag chains not being restricted to the nearest neighbors indicates that electrons are not fully localized in the COS phase as well. The large and non-local ferro-magnetic interactions in the zigzag chains yield considerable resemblance between the COS and the metallic phases. This resemblance might be essential to understand the capability of manganites to switch between the metallic ferromagnetic and the insulating COS phases. These results have been published in reference [6].

[1] Y. Tokura and N. Nagaosa, Science **288**, 462 (2000).

[2] Y. Motome et al., Phys. Rev. Lett. **91**, 167204 (2003).

[3] E.O.Wollan and W.C. Koehler, Phys. Rev. **100**, 545 (1955).

[4] J.B. Goodenough , Phys. Rev. **100**, 564 (1955).

[5] Y. Endoh et al., Phys. Rev. Lett. **94**, 017206 (2005).

[6] D. Senff, F. Krüger, S. Scheidl, M. Benomar, Y. Sidis, F. Demmel and M. Braden, Phys. Rev. Lett. **96**, 257201 (2006).

H6. COMPETING ORDER PARAMETERS IN LIGHT-RARE-EARTH HEXABORIDES

J.-M. MIGNOT[1], G. ANDRÉ[1], M. SERA[2], AND F. IGA[2]

[1] Laboratoire Léon Brillouin (CEA-CNRS), CEA/Saclay, 91191 Gif sur Yvette Cedex
[2] ADSM, Hiroshima University, Higashi Hiroshima, 739-8530, Japan

Orbital phenomena associated with *d* electron states are known to be central to the physics of transition-metal oxides, and have been extensively studied. In the case of *f* electrons, which are subject to strong spin-orbit coupling, the proper description of orbital degrees of freedom is based on *multipoles*. Ordering phenomena involving higher-rank multipoles (quadrupoles, octu-poles, etc.) are currently attracting a great deal of interest, because they might account for several elusive phase transitions observed in rare-earth or actinide compounds ($Ce_{1-x}La_xB_6$, $SmRu_4P_{12}$, NpO_2, etc.). Multipole moments, being tensor quantities, can give rise to a variety of ordered states classified according to the symmetry of their order parameter. Interesting properties are expected to occur if a competition takes place between different types of order, involving multipole components of different symmetries. Such a situation may be realized in the cubic (CsCl-type) hexaboride compounds $Ce_{1-x}R_xB^6$ (*R*: Pr, Nd), where the light rare-earth Ce, Pr, and Nd have different mul-tiplet ground states (*J* = 5/2, 4, and 9/2, respectively), and thus different multipole moments.

CeB_6 is considered the archetype of a pure antiferro-quadrupolar (AFQ) order, realized in the so-called "phase II" below T_Q = 3.2 K, prior to the onset of a long-range magnetic order in "phase III" below T_N = 2.3 K [1]. In the latter phase, the Ce magnetic moments form a noncollinear, planar, 2*k*-*k*' structure, described by the 4 propagation vectors $\boldsymbol{k}_{1,2}$ = (1/4, ±1/4, 1/2) and $\boldsymbol{k}'_{1,2}$ = (1/4, ±1/4, 0). The preformed order of the O_{xy} (O_{yz}, O_{zx}) quadrupole moment components, with the wave vector $\boldsymbol{k}_Q$ = (1/2,1/2,1/2), produces a staggered anisotropy on the Ce sublattice, which is thought to be responsible for the unusual type of magnetic structure adopted by the system below T_N. Substitution of another rare earth ion (including La) strongly suppresses phase II, giving way to a rich pattern of ordered phases as a function of both concentration (Fig. 1) and applied magnetic field. Most of these phases have a clear magnetic signature, but quadrupole, and possibly higher multipole couplings are likely to play a role. The present study aims at understanding the microscopic mecha-nisms responsible for the stability of the different structures. Neutron diffraction measurements have been reported in Refs. [3,4] for $Ce_{1-x}Pr_xB_6$ and $Ce_{1-x}Nd_xB_6$, respectively. Here we present our results for the latter system, together with a brief discussion of their implica-tions as to a possible role of quadrupole interactions.

Powder and single-crystal experiments were performed on the multidetector diffractometer G4-1 and the lifting-counter diffractometer 6T2, using isotopic (^{11}B: 98.6%) samples prepared in Hiroshima.

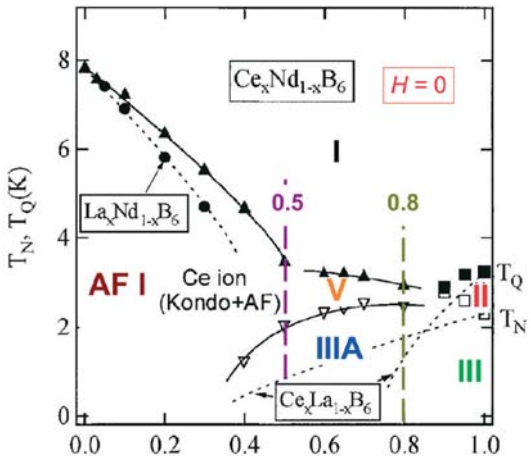

Figure 1. Phase diagram of $Ce_{1-x}Nd_xB_6$ in zero applied magnetic field; the vertical dashed lines cor-re-spond to the concentrations studied experimen-tally; $Ce_{1-x}La_xB_6$ data are plotted for comparison. (after Ref. [2])

The powder diffraction patterns (Fig. 2) reveal two clearly distinct regimes. For *x* = 0.5, the systems first orders below T_N in a simple AFI structure $\boldsymbol{k}_{AFI}$ = (0,0,1/2), similar to that found in pure NdB_6. Resistivity measurements suggest that, in this regime, the Ce ions are weakly coupled to the Nd magnetism and retain Kondo fluctuations inside the AFI ordered state. The fact that the 0 0 1/2 reflection is absent implies that the moment direction is parallel to the fourfold axis, pointing to an effect of ferroquadrupolar O^0_2 -type inter-actions between Nd moments as in pure NdB_6 [5]. For *x* = 0.8 (Fig. 2, upper frame), the structure forming below T_N is incommensurate with $\boldsymbol{k}_{inc}$ = (0.237, 0.237, 1/2). At lower temperature, a lock-in transition takes place to the commensurate (C) wave vector $\boldsymbol{k}_{com}$ = (1/4, 1/4, 1/2).

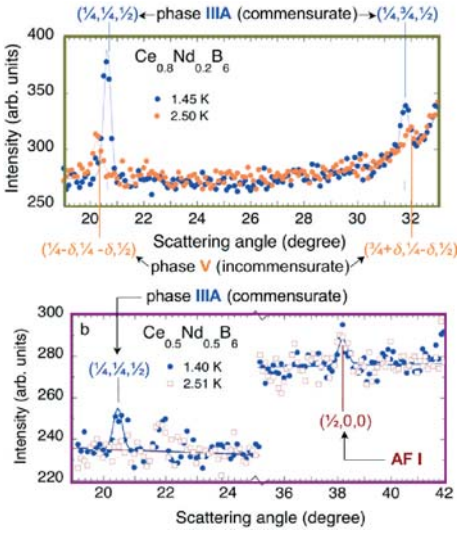

Figure 2. Powder diffraction patterns for $Ce_{1-x}Nd_xB_6$ (*x* = 0.8 and 0.5) mea-sured in the ground state at T_{min}⊕[a] 1.4 K and in the intermediate phase below T_N.

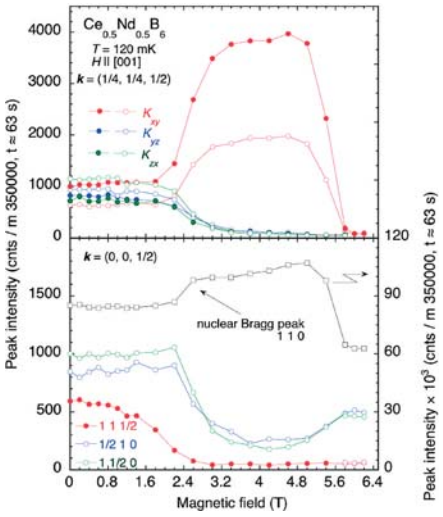

Figure 3. Field dependence of Bragg intensities for different C (upper frame) and AFI (lower frame) satellites at T = 120 mK.

This situation in phase IIIA is reminiscent of the compound PrB_6, where the structure was analyzed as 2-*k* and ascribed to an effect of quadrupole interac-tions between O_{xy}-type moments. The absence of ***k'***-type peaks, in contrast to the CeB_6 case, reflects the lack of long-range AFQ order associ-ated with $\boldsymbol{k}_Q$.

In the Nd-rich compound x = 0.5, the low-temperature transition again corresponds to the appearance of a commensurate component at $\boldsymbol{k}_{com}$ but, in this case, the high-temperature AFI reflections are not suppressed (Fig. 2, lower frame), suggesting that ordering behaviors associated with Ce and Nd moments somehow coexist.

This assumption is supported by the single-crystal results. At the lowest temperature of T = 120 mK, the intensity of the AFI peak 1 1/2 0 is indeed comparable to that of the C satellite 5/4 1/2 1/4. When an external field is applied along [001], the intensities plotted in Fig. 3 indicate a repopulation of the C domains above $H_1 \oplus 2.4$ T (upper frame), consistent with the hypothesized 2-*k* planar, PrB_6-like structure. More surprisingly, this change is accompanied by a steep suppression of the Bragg peaks associated with the AFI single-*k* domains k_x and k_y (lower frame). Those associated with k_z, on the contrary, decrease smoothly to zero from H = 0 to 2.4 T. This leads us to propose that the AFI (k_x and k_y) and C (k^c_{y2} and k^c_{2x}) components are actually coupled by pairs (e.g. k^c_{y2} with k^c_x), and contribute to one and the same structure within a given domain. We further speculate that the two components may reflect, respectively, the Ce and Nd contributions, with Ce moments forming a structure similar to the planar 2-*k* state mentioned above, and Nd moments an approximately AFI state along the normal to the planes. In this picture, the

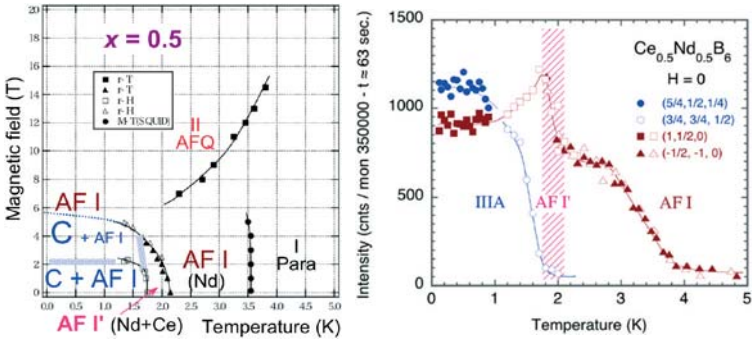

Figure. 4. (*left*): (H,T) magnetic phase diagram of $Ce_{0.5}Nd_{0.5}B_6$ (data for bulk measurements from Kawaguchi et al.). (*right*): T dependences of the intensities of C and AFI satellites at H = 0.

effect in low fields implies no true domain repopulation but a mere reorien-tation of the Nd moments within the k^c_{xy} - k_z domain.

Above a second transition field H_2 = 5.4 T, the C structure is steeply suppressed, and AFI order is restored, with only the two domains k_y and k_z populated. This is consistent with moments oriented, within each domain, along the propagation vector. In high fields, no evidence was found for the AFQ transition line derived from bulk measurements. The results in applied fields are summarized by the phase diagram drawn in Fig. 4.

Finally, we want to point out the interesting observation of an intermediate region in the phase diagram, between 1.7 and 2.5 K in zero field, which is characterized by a steep increase in the AFI component just before the C order sets in. We believe that it denotes the ordering of Ce moments in the existing AFI structure of Nd, likely associated with the suppression of Kondo fluctuations.

In conclusion, the complex pattern of ordered phases found in the $Ce_{1-x}Nd_xB_6$ solid solutions appears to reflect the rather unique competition of two different types of quadrupolar couplings, predominantly FQ between the Nd O^0_2 moments, and AFQ between the Ce O_{xy}-type moments. Neutron diffraction under conditions of high magnetic fields and very low temperatures has proved invaluable in revealing the details of the magnetic phases. It should now be complemented by x-ray synchrotron measurements to probe directly the order of multipole moments.

[1] J.M. Effantin, J. Rossat-Mignod, P. Burlet, *et al.*, J. Magn. Magn. Mater. 47&48 (1985) 145.

[2] S. Kobayashi, Y. Yoshino, S. Tsuji, M. Sera, F. Iga, J. Phys. Soc. Jpn. 72 (2003) 25.

[3] J.M. Mignot, M. Sera, F. Iga, Physica B 383 (2006) 41.

[4] J.M. Mignot, G. André, M. Sera, F. Iga, Physica B (in press).

[5] S. Awaji, N. Kobayashi, S. Sakatsume, S. Kunii, M. Sera, J. Phys. Soc. Jpn. 68 (1999) 2518.

H7. SPIN REDISTRIBUTION BY ENTANGLEMENT IN AN ORGANIC MAGNET

A. ZHELUDEV[1], V. O. GARLEA[1], S. NISHIHARA[2], Y. HOSOKOSHI[3], A. COUSSON[4], A. GUKASOV[4], K. INOUE[5]

[1]HFIR Center for Neutron Scattering, Oak Ridge National Laboratory, Oak Ridge, TN 37831-6393, USA.
[2]Department of Physical Science, Osaka Prefecture University, ,Osaka 599-8531, Japan.
[3]Department of Physical Science, Osaka Prefecture University, Osaka 599-8531, Japan; Institute for Nanofabrication Research, Osaka Prefecture University, Osaka 599-8531, Japan.
[4]Laboratoire Leon Brillouin, CEA-CNRS Saclay, France.
[5]Department of Chemistry, Hiroshima University, Hiroshima 739-8526, Japan.

A fundamental feature of quantum mechanics is entanglement, defined as a physical realization of linear superpositions of simple multi-particle states [1]. Entangled particles are physically interdependent even though they may be spatially separated. Entanglement of spin degrees of freedom in molecular magnets holds great promise for spintronics devices [2]. Rather complex entangled states are realized in applied magnetic fields. For each magnetic group of atoms the spin is quantized, and the magnetization can have only discrete values. Due to entanglement though, the spin density can be arbitrarily re-distributed, resulting in seemingly paradoxical fractional local magnetization. Recent experiments on the 5C1 and 6T2 [6] polarized neutron diffractometers at the ORPHEE reactor yielded a direct quantifiable experimental observation of this effect in a novel organic molecular magnet.

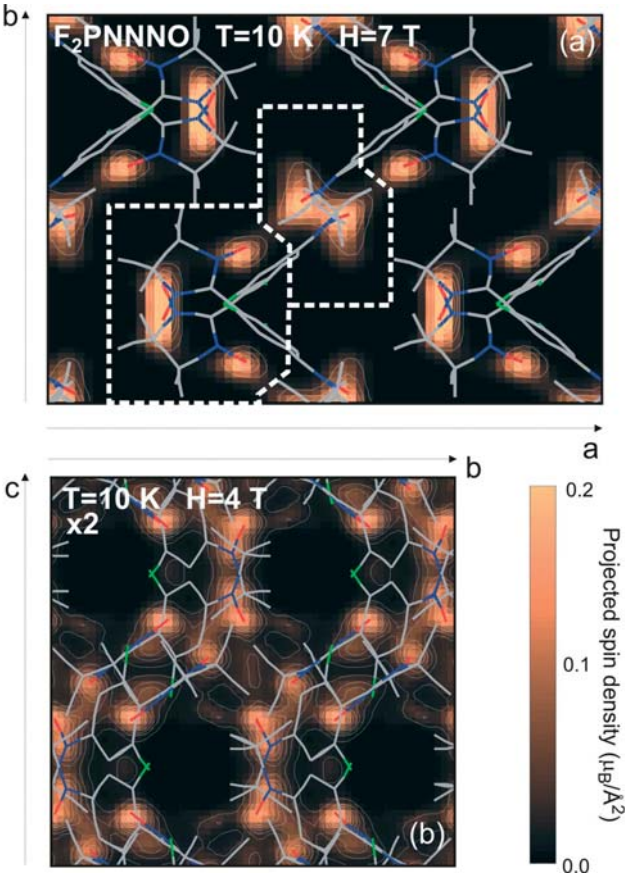

Figure. 1. Experimental spin density distribution in a F_2PNNNO spin-tetramer at T = 10 K, as reconstructed using the Maximum Entropy method. Areas outlined with thick dashed lines were used to estimate the spin populations on the nitronyl nitroxide and *tert*-butyl nitroxide.

Our model material, 2-[2,6- difluoro -4-(*N-tert-* butyl-*N-* oxyamino) phenyl] -4,4,5,5 – tetramethyl -4,5 – dihydro -1 *H*-imidazol -1-oxyl 3-oxide, F_2PNNNO for short, is a prototypical spin tetramer system [3]. The magnetic properties are due to two unpaired electrons that reside in p* antibonding molecular orbitals of the nitronyl nitroxide (NN) and the *tert*-butyl nitroxide (tBuNO) groups, respectively. These S = 1/2 spins are coupled via a ferromagnetic intramolecular exchange constant J_F ~ 35 meV.

When in crystalline form, F_2PNNNO molecules are arranged in pairs, so that their tBuNO groups are close enough for AF interactions of magnitude J^{AF} ~5.8 meV. The result is a two-molecule unit containing four interacting spins. Its unique ground state is a non-magnetic singlet. In the presence of an external magnetic field applied along the z axis, the excited state with the lowest energy has a total spin S_{total} = 1 and a spin projection S_z = +1. We shall denote this state as $|1,+1\rangle$. Its wave function is heavily entangled : by diagonalizing the Heisenberg Hamiltonian of the tetramer we find that it actually is a linear combination of four ``pure'' (non-entangled) spin wave functions: $|1,+1\rangle = a|\_\_\_\_\rangle + b|\_\_\_\_\rangle - a|\_\_\_\_\rangle - b|\_\_\_\_\rangle$, where a ~ 0.46 and b ~ 0.54. The most striking consequence of this entanglement is an imbalanced spin density distribution $S_z(\boldsymbol{r})$: the local spin populations of the NN groups are equal, but different from those of the tBuNO groups. The ratio R of these spin populations is given by $R = a^2/b^2$ ~ 1.39. If entanglement was absent, and only pure spin-projection states were allowed, then, due to the weakness of the central antiferromagnetic bond, the lowest-energy excited state would have been $|\_\_\_\_\rangle$, with R_{pure} = 1. If quantum mechanics failed altogether, the spins would behave as classical moments. They would align themselves in the (x,y) plane and tilt slightly in the field direction. It is easy to show that the resulting imbalance in $S_z(\boldsymbol{r})$ would be minuscule: $R_{classical} = 1+|J_{AF}|/4|J_F| = 1.04$. Thus, a large imbalance of NN and tBuNO spin densities in F_2PNNNO can be considered a *signature of spin entanglement*.

To prepare the tetramer in its $|1,+1\rangle$ excited state high magnetic fields of H = 7 T or H = 4 T were used to lower its energy as much as possible. The data were then taken at an elevated temperature of T = 10 K that made this state partially populated. The main technical challenge of measuring the spin density distribution is the very small total magnetization, estimated at less than half a Bohr magneton for the 2-molecule unit comprising about 100 atoms. Polarized neutron in the crystal.

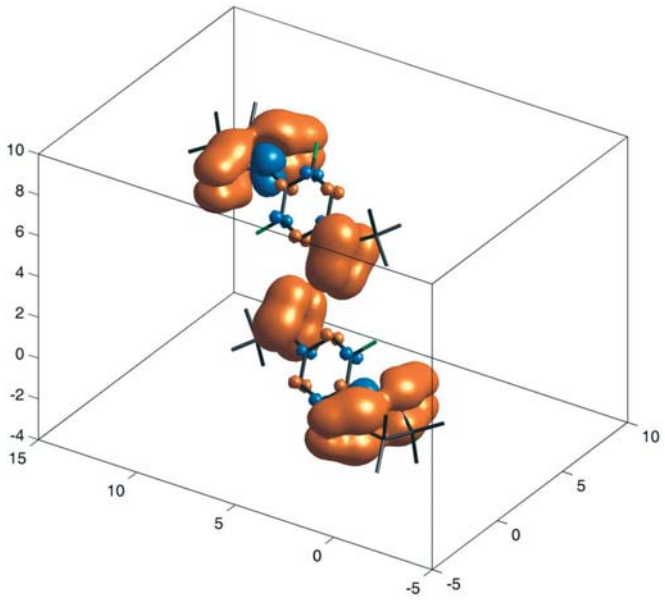

Figure. 2 Experimental spin density distribution in a F2PNNNO spin-tetramer at T = 10 K at H = 7 T and T = 10 K, as reconstructed using atomic orbital expannsion. The isosurfaces are drawn at 1x10-3 $_{\mu B}$/Å^3 (orange) and -1x10-3 $_{\mu B}$/Å^3 (blue) levels. The axes show Cartesian coordinates in Angstroms.

In the experiments the so-called flipping ratios of 70 Bragg reflections were measured. Maximum entropy (Fig. 1) and atomic orbital expansion (AOE, Fig. 2) were used to reconstruct the real-space magnetization distribution.

A very good measure of the reliability of the AOE reconstruction is its result for the total tetramer magnetization: m = 0.48(2) μ_B and m = 0.28(2) μ_B, for H = 7 T and H = 4 T, respectively. These values are consistent with existing bulk susceptibility data, and are in excellent agreement with a thermodynamic quantum-mechanical calculation for a single tetramer: m = 0.59 μ_B and m = 0.32 μ_B, respectively. With this assurance of the validity of our approach, we obtain experimental estimates for the imbalance between the NN and tBuNO spin populations: R = 1.53(3) and R = 1.51(2), for H = 7 T and H = 4 T. The quantitative agreement with theoretical predictions for entanglement-induced spin redistribution in F_2PNNNO is remarkable.

Our polarized neutron diffraction results not only provide a direct evidence of spin entanglement, but also help understand the microscopic interactions that cause it. In Fig. 2, note the negative density in the vicinity of the apical carbon atom of the NN group. This large negative spin population [4] plays a key role in the ferromagnetic intra-molecular coupling J_F. It is a part of a sign-alternating spin density wave that propagates across the phenyl ring and connects the positively populated N sites of the NN and tBuNO fragments over a large distance. This density-wave mechanism is analogous to Ruderman-Kittel-Kasuya-Yosida interactions in metals. AF interactions J_{AF} between tBuNO groups of the two molecules comprising each tetramer span a shorter distance, and are more conventional in nature. They are due to direct exchange and arise from molecular orbital overlap.

The simplicity and isotropic nature of delocalized magnetic *sp*-electrons in organic molecules make them useful as a testing ground for fundamental quantum mechanics. In the particular case of F_2PNNNO we are able to detect and precisely quantify the redistribution of spin density caused by entanglement of four interacting quantum spins, and learn about the microscopic mechanisms of these entangling interactions.

A full report on this study can be found in Ref. [5].

[1] Mermin, N. D., Physics Today **38**, 38 (1985).

[2] Leuenberger, M. N. and Loss, D., Nature **410**, 789 (2001).

[3] Hosokoshi, Y., Nakazawa, Y. and Inoue, K., Phys. Rev. B **60**, 12924 (1999).

[4] Davis, M. S., Morokuma, K. and Kreilick, R. W., J. Am. Chem. Soc. **94**, 5588 (1972).

[5] A. Zheludev, V. O. Garlea, S. Nishihara, Y. Hosokoshi, A. Cousson, A. Gukasov and K. Inoue, cond-mat/0609299.

[6] A. Gukasov, A. Goujon, J.-L. Meuriot, C. Person, G. Exil and G. Koskas, Physica B, *Proceedings of PNCMI-2006*, Berlin (see also in this report).

[*C1*. S. P. Bayrakci] Magnetic Ordering and SpinWaves in $Na_{0.82}CoO_2$

Na_xCoO_2, the parent compound of the recently synthesized superconductor $Na_xCoO_2=(H_2O)_y$, exhibits bulk antiferromagnetic order below ~20 K for 0.75 < *x* < 0.9, y = 0. We have performed neutron scattering experiments on a $Na_{0.82}CoO_2$ single crystal and observed for the first time Bragg reflections corresponding to A-type antiferromagnetic (AF) order (i.e. ferromagnetic *ab*-planes antiferromagnetically coupled along the *c* axis). The magnetic order is characterized by magnetic moments directed along *c** axis, causing the elastic neutron scattering cross section to vanish for purely magnetic Bragg reflections such as ***Q*** = (0,0,1) (see figure). On other Bragg reflections, both nuclear and magnetic signals are superimposed, and polarized neutron scattering technique becomes essential to extract the weak magnetic signal. After calibrating the magnetic intensity measured for Q = (1,0,1) against the intensity of the (1,0,0) nuclear peak, we could extract a value of the ordered magnetic moment equal to 0.13 ± 0.02 mB per Co atom. The observation of transverse magnetic excitations along the c* direction was comparatively straightforward and the results can be perfectly described by the standard spin-wave theory. However, both the weakness of the ordered magnetic moments and the damping of the spin-wave excitations suggest that $Na_{0.82}CoO_2$ may correspond to an itinerant magnetic system.

[Collaboration : S. P. Bayrakci, B. Keimer, D. P. Chen, C. T. Lin, MPI Stuttgart – I. Mirebeau, Ph. Bourges, Y. Sidis, LLB – M. Enderle, ILL – J. Mesot, PSI]

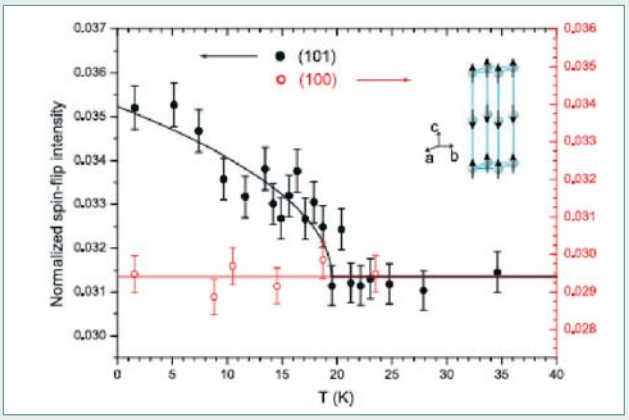

S. P. Bayrakci et al., Phys. Rev. Lett. **94**, 157205 (2005)

Normalized spin-flip intensity for ***Q*** = (1,0,1) and (1,0,0) plotted as a function of temperature. The data were taken with the neutron polarization ***P*** // ***Q***, at an incident neutron energy of E_i = 14.7 meV. The lines are guides to the eye. Inset: *A*-type AF structure, represented with Co spins // *c*

[*C2*. O. Mentré] Spin gap in the one-dimensional S = 1/2 spin-ladder compound $Bi_2Cu(P_{1-x}V_x)O_6$

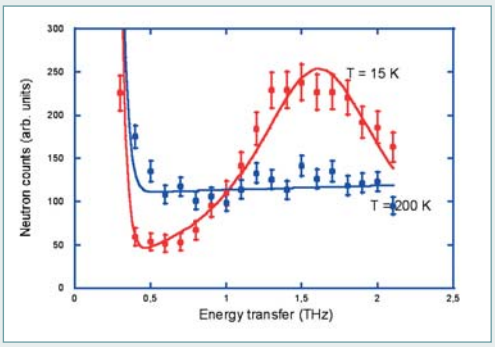

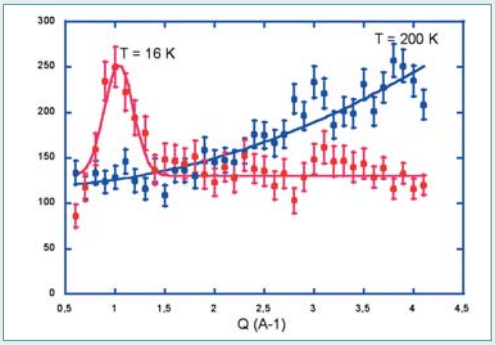

Spin ladders, spin-Peierls, or more generally dimer-chain systems have proven to be a very rich subject because of their essential quantum nature, at the crossroad between one and two dimensions. $Bi_2Cu(P_{1-x}V_x)O_6$ belongs to this new interesting class of materials. The analysis of its crystallographic structure shows that the copper ions, carrying an *S* = 1/2 spin, form zigzag two-legs ladders running along the *c* axis, with rungs parallel to the *b* direction. Two adjacent ladders are separated by nonmagnetic Bi ions and PO_4 and VO_4 groups, depending on the substitution level *x*. These PO_4 and VO_4 groups strongly affect the competition between magnetic couplings along the legs, along the rungs, and between adjacent ladders, leading in turn to different ground states. These structural properties are closely related to the spin dynamics. The evolution of the spin susceptibility as a function of temperature is typical of a spin-gap system for *x* < 0.7, while this spin-gap behaviour is lost for 0.7 < *x* < 1 . Inelastic neutron scattering measurements performed on powder samples with *x* = 0, 0.6, 0.9, and 1 enabled us to directly measure this spin gap for *x* = 0 and 0.6. The figures show typical w scans performed at fixed Q = 1 $Å^{-1}$ [above], and typical ω scans performed at fixed energy transfer ω = 1.5 THz (6 meV) [under]. Cooling down to 15 K unambiguously shows the appearance of dynamical correlations peaked around Q = 1 A^{-1}, which corresponds to half the distance between copper spins. Further investigations on single crystals are planned to improve the description of the magnetic response.

[Collaboration : O. Mentré, F. Leclercq Hugueux (LPCS, ENSCL, Villeneuve d'Ascq) S. Petit, M. Hennion (LLB)]

[*C3*. S.M. Yusuf] Two- and three-dimensional magnetic ordering in the bilayer manganite $Ca_{2.5}Sr_{0.5}GaMn_2O_8$

This neutron diffraction study on the bilayered manganite $Ca_{2.5}Sr_{0.5}GaMn_2O_8$ has revealed a crossover phenomenon – from 3D short-range (SR) to 2D long-range (LR), then to restricted 3D LR (RLR), and finally to true 3D LR – in the antiferromagnetic correlations between the [010] oriented Mn spins in the *a-c* plane (Figs. *a-c*). The effect takes place over a wide temperature range. Here 3*d* magnetism and superexchange interactions are involved. The observation of a marked decrease in the resistivity on cooling and of a large negative magnetoresistance (~50 %) near the 3D LR Néel temperature suggest that the electronic and magnetic properties are strongly coupled and dimension-dependent. The present study is therefore highly relevant to the ongoing search for new 2D materials in the field of spintronics.

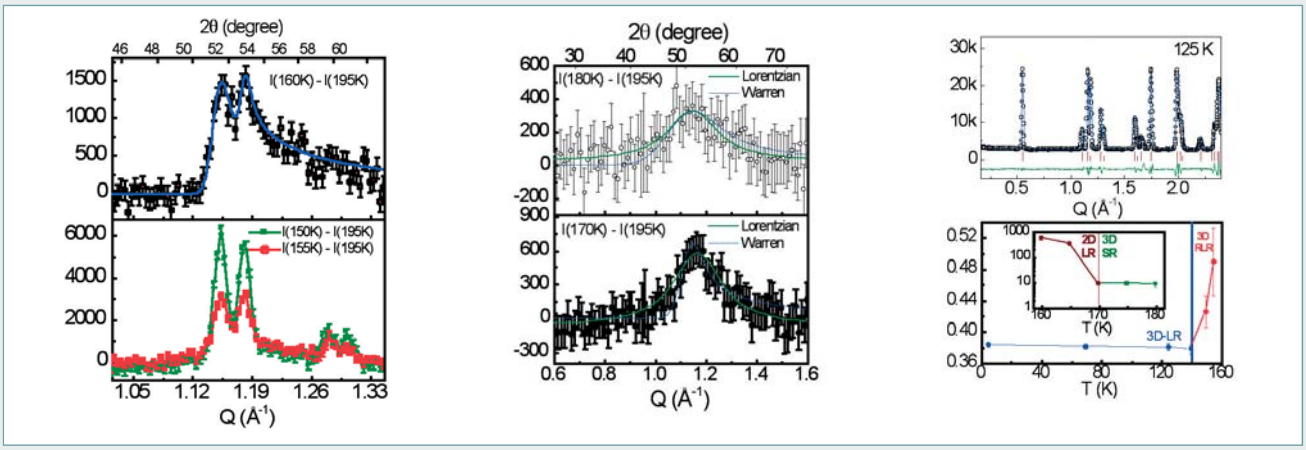

(a) Magnetic neutron diffraction patterns at 160, 155 and 150 K; nuclear background at 195 K has been subtracted out. The solid curve in the upper panel is a calculated profile using the 2D Warren function; in the bottom panel, lines are guides to the eye. **(b)** Magnetic diffraction patterns at 180 and 170 K ; solid curves are calculated profiles using 2D Warren functions and 3D Lorentzian functions. **(c)** Top: Rietveld-refined neutron diffraction patterns at 125 K; bottom: half width at half maximum (HWHM), averaged for the 3D Bragg peaks (100) and (001). Inset: temperature dependence of the spin-spin correlation length _.
[Collaboration: S.M. Yusuf, M. D. Mukadam, Bhabha Atomic Research Centre, India; J. M. De Teresa, P. A. Algarabel, C. Marquina, and M. R. Ibarra, Universidad de Zaragoza-CSIC, Spain; I. Mirebeau, J.-M. Mignot, LLB]

[*C4*. C. Aronica] Ferromagnetic Interaction in an Asymmetric End-to-End Azido Double-Bridged Copper(II) Dinuclear Complex

The nature of the intramolecular magnetic coupling in azido double-bridged copper(II) dinuclear complexes appears to be highly correlated to the coordination mode of the bridging azido (N3) groups. As a matter of fact, almost all the End-On complexes (›N-N-N bridging mode) present a triplet ground state (S = 1) while the majority of End-to-End complexes (-N-N-N- bridging mode) either display a singlet ground state (S = 0), or behave as two independent spins _. A new End-to-End azido-bridged copper(II) complex $[Cu_2L_2(N_3)_2]$, with L : 1,1,1-trifluoro-7-(dimethylamino)-4-methyl-5-aza-3-hepten-2-onato, has been synthesized and characterized. Despite the rather long Cu–Cu distance (5.105(1)Å) measured from the x-ray diffraction crystal structure determination, the magnetic interaction is ferromagnetic with J = +16 cm-1 ($H = -J\, S_1 S_2$). The experimental spin distribution from polarized neutron diffraction has been found to be localized mainly on the Cu(II) ions. Small delocalization has been observed on the ligand (L) and terminal azido nitrogen atoms, whilst it is strictly zero on the central nitrogen. Such a picture denotes a large contribution of the $d_{x^2-y^2}$ orbital (in the CuN_2N_5 plane) and a small population of the d_{z^2} orbital (along the Cu-N3 direction), in agreement with our calculations.
[C. Aronica, E. Jeanneau, D. Luneau, H. El Moll, G. Pilet, Laboratoire des Multimatériaux et Interfaces, Villeurbanne; M. A. Carvajal, V. Robert, Laboratoire de Chimie, ENS Lyon; B. Gillon, A. Goujon, A. Cousson, LLB]

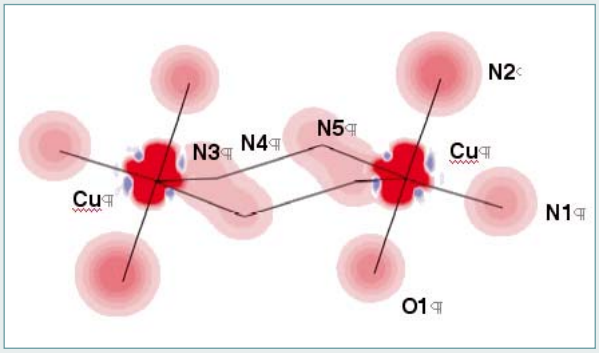

Experimental induced spin density in $[Cu_2L_2(N_3)_2]$ at 2 K and H = 5 T projected along the b axis. Low levels only are represented: from 0.02 mB/Å² to 0.1 mB/Å² by steps of 0.02 μ_B/Å².

[C5. J. Manson] Neutron diffraction study of a molecule-based 2-dimensional magnetic compound $Mn(dca)_2(pym)(H_2O)$: spin density and magnetic phase diagram.

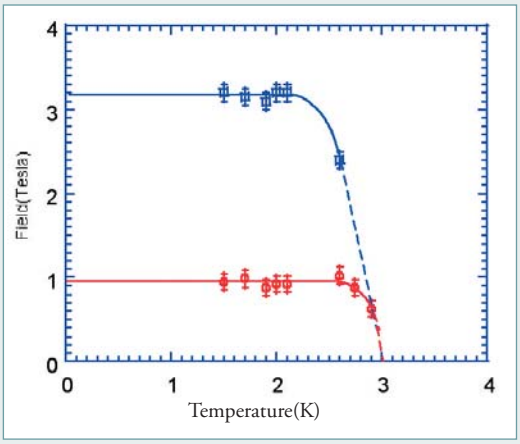

Figure 1. Magnetic phase diagram (H,T) of $Mn(dca)_2(pym)(H_2O)$.

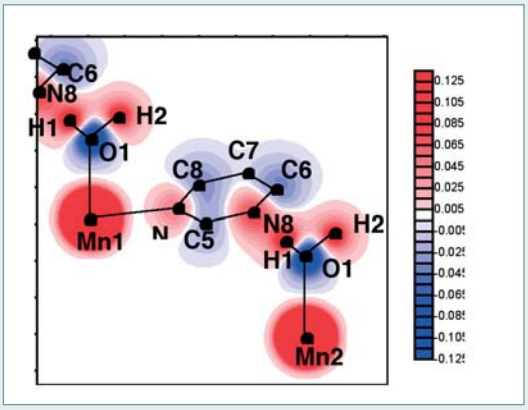

Figure 2. Induced spin density projection along the perpendicular to the O1H1N8 plane at 5 K under 4.5 T

The $Mn^{II}(dca)_2(pym)(H_2O)$ compound (with dca = $N(CN)_2$ and pym = $N_2C_4H_4$) presents a 2-dimensionnal structure formed by layers in which the Mn^{2+} ions are alternately related by single or double (-NC-N-CN-) dicyanamide bridges. These layers, stacked along the *c*-axis, are connected by hydrogen bonds between the coordinated water molecules and N atoms of the pyrimidine rings and of the dicyanamide groups. The magnetic phase diagram established by single-crystal diffraction is reported in Fig. 1. In the AF1 structure, the antiferromagnetic ordered Mn^{2+} layers are AF-coupled to each other, while in the AF2 phase, above the spin flop transition, the layers are ferromagnetically coupled. In order to investigate the magnetic interaction pathways in this compound, particularly between the layers, the induced spin density has been determined by polarised neutron diffraction in the paramagnetic state at 5 K under a field of 4.5 T. The spin density map shown in Fig. 2 clearly evidences a positive spin density on the hydrogen atom of the N8..H1-O1 hydrogen bond, which overlaps with the positive density of the nitrogen atom N8 of the pyrimidine ring. This overlap favors AF coupling between the layers in zero field.

[Collaboration: J. Manson, Department of Chemistry and Biochemistry, Eastern Washington University, USA; B. Gillon, A. Gukasov, A. Cousson, LLB]

[C.6. A. Goujon] Photoswitchable molecular compounds studied by neutron powder diffraction.

Determining the magnetic structure of photoswitchable magnets is a main goal to understand the mechanism of photo-excitation. Neutron powder diffraction reveals the magnetic structure of compounds and provides an understanding of magnetic and structural correlations (nature, length scale). A dedicated sample holder has been designed to allow photoexcitation measurements to be performed *in situ* on the powder spectrometer G4-1. Ancillary equipments, such as a pulsed laser (Nd:YAG, *Minilite II*) or optical fibers, were also installed on G4-1. The design of the sample holder takes into account the need *(i)* to work with about 1 g of powder, and *(ii)* to illuminate homogeneously the majority of the powder in order to induce sizeable photo-conversion. Photoexcitation of a $[Fe_{0.52}Zn_{0.48}(btr)_2(NCS)_2](H_2O)$ powder was carried out at 15 K using a pulsed laser light (λ = 532 nm). At low temperature, the spin conversion is easily obtained by LIESST (light-induced excited spin state trapping) effect, and accompanied by huge structural changes. Fig. 1 shows a comparison between the low-spin (LS) state spectrum and the photoinduced state obtained after 20 hours. A mixing of the LS and photoinduced HS fractions was evidenced, indicating that 30% of the sample was converted to the HS state. The kinetics of the photoexcitation is shown in Fig. 2. The partial photoconversion is well explained by the strong absorption of the powder. This result is encouraging and further work is underway to increase the yield of photoexcitation.

[A. Goujon, B. Gillon, G. André, A. Gukasov, LLB]

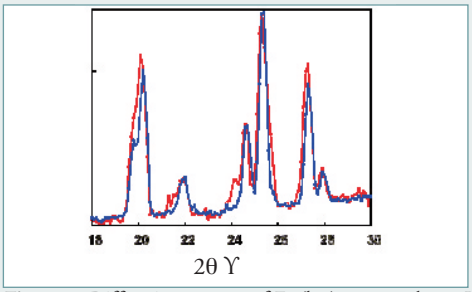

Figure 1. Diffraction pattern of Fe (btr) measured at 2 K (blue): LS state; (red): after 20 hours of photoexcitation.

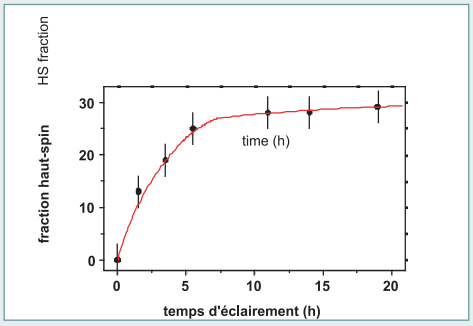

Figure 2. Kinetics of the photoexcitation in In $[Fe_{0.52}Zn_{0.48}(btr)_2(NCS)_2](H^2O)$ at T = 15 K.

[*C7.* A. Goujon] Neutron Laue diffraction on the spin crossover crystal $[Fe(ptz)_6](BF_4)_2$ showing continuous photo-induced transformation

Structural aspects of photoinduced phase transitions in spin-crossover compounds have been investigated by neutron Laue diffraction. A photocrystallographic experimental setup has been installed on the vertical-axis Laue diffracto-meter VIVALDI at the Institut Laue Langevin. The structures of the ground state and of the metastable LIESST (Light Induced Excited Spin State Trapping) state of the Fe^{II} spin-transition compound $[Fe(ptz)_6](BF_4)_2$ in the quenched state were determined at T = 2 K. The results show that the local structure change upon photoinduced spin transformation is essentially an expansion of the $Fe\text{-}N_6$ core without lowering of the O_h symmetry of the Fe environment. The Fe–N distance is increased by 0.21 Å and the unit-cell volume by about 2%. It was found that the local structure of the photoinduced phase is very close to that of the high-temperature high-spin state. The evolution of the (0,-2, 8) Laue spot, as a function of the total irradiation time, is shown in the figure. For the first time, a progressive character of the photoinduced phase transformation was evidenced in spin-crossover compounds. The observed continuous shift clearly rules out the nucleation and growth of like-spin domains (LSDs) in the phase transformation. It also shows the basically homogeneous character of the photoexcitation process.

[A. Goujon, B. Gillon, A. Cousson, A. Gukasov, LLB; F. Varret, GEMAC, Versailles; G. McIntyre, ILL, Grenoble]

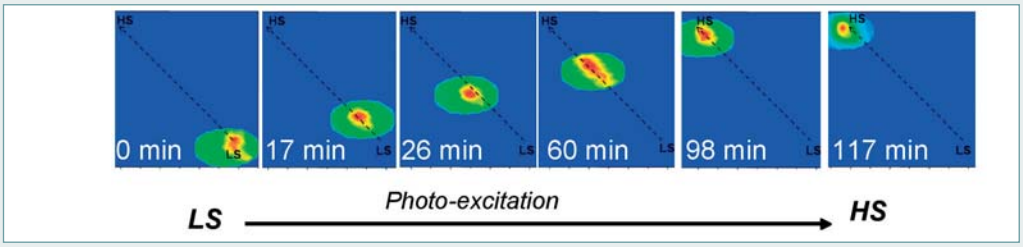

Absence of LSDs during photo-excitation of the spin-crossover crystal $[Fe(ptz)_6]BF_4$, rhombohedral phase (Goujon et al., Phys. Rev. B, 2006)

[*C8.* A. Tamion] Magnetization depth profile of (Fe/Dy) multilayers

The magnetization of [Fe 3nm/Dy 2nm] multilayers has been studied. The samples were thermally evaporated under ultra-high vacuum at different substrate temperatures varying from 320 K to 870 K. In order to get the magnetization depth profile of these Transition Metal/Rare Earth (TM/RE) multilayers, an investigation of the structural, chemical, and magnetic properties was carried out. The samples were studied by High Resolution Transmission Electron Microscopy (HRTEM), Three-Dimensional Atom Probe (3DAP) and Polarized Neutron Reflectivity (PNR). The multilayers have been found to be rather homogeneous, except for the first two bilayers deposited on the substrate : the mainly crystalline structure of the first Fe layers leads to an enhancement of the ordering temperature of amorphous Dy. Moreover, at low temperature, a negative exchange coupling between Fe and Dy layers has been evidenced. Magnetization profiles have also been calculated by Monte Carlo simulations to support the PNR fits.

[Collaboration : A. Tamion, P.-E. Berche, E. Talbot, C. Bordel and D. Blavette (Université de Rouen), F. Ott (LLB)

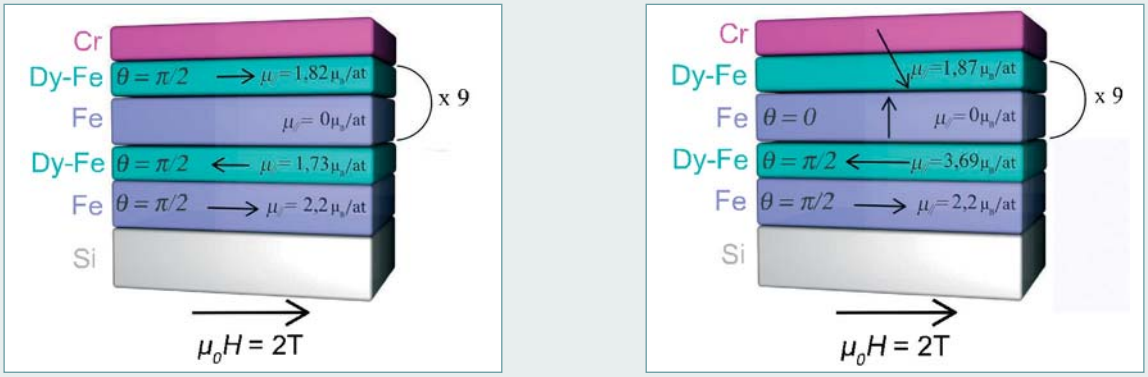

Samples deposited at a substrate temperature of 570 K. There is some interdiffusion between the Fe and the Dy layers. (left) at room temperature, no moment was found in the Fe layer because of its amorphous nature; (right) at 100 K, the Fe and Dy-Fe layers order antiferromagnetically. The layers in contact with the substrate behave very differently from the top layers.

[*C9.* M. Delalande] Polarized SANS studies of FePt Magnetic Nanoparticles

Small angle neutron scattering with polarized neutrons (SANSPOL) has been performed on films of FePt nanoparticles prepared by first diluting the powder in deuterated toluene (0.1% volume concentration) then drying it out. Magnetization measurements show a superparamagnetic behavior below 25 K. The saturated magnetization is 290 emu/cm^3, about 25% of the value for bulk FePt. The particle size distribution is centered around 4.8 nm (left frame) with a 10% dispersion. SANSPOL data taken at T = 5 K in an applied field of H = 2.1 T (right frame) exhibit a peak at around 0.8 nm^{-1} indicative of an inter-particle distance of about 8 nm. This is in agreement with a picture of particles of diameter 5 nm linked by organic molecules of length 3 nm. As the temperature is increased a slight shortening of the inter-particles distance is observed.

[Collaboration: M. Delalande, A. Marty (DRFMC, CEA Grenoble); G. Chaboussant, S. Gautrot (LLB)]

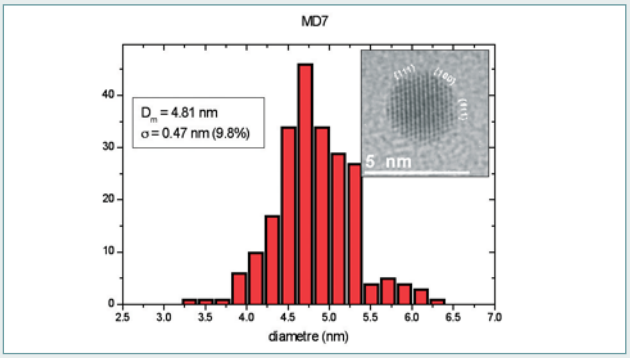

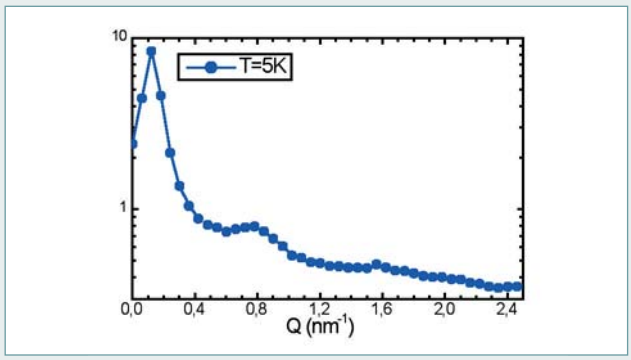

(left): Size distribution and TEM image of 5nm FePt particles. **(right):** SANSPOL data ($\Delta I = I^+ - I^-$) of FePt particles at 5 K in a field of 2.1 T. The inset shows the2D SANS signal; the ring structure reveals a magnetic contribution at $Q \approx 0.8$ nm^{-1}.

[*C10.* G. Viau] Small Angle polarised neutrons studies of dispersed magnetic Co-Ni nanowires

Small angle neutron scattering with neutron polarisation (SANSPOL) has been performed on dispersed magnetic nanowires presenting a wide range of sizes and shapes. The length range from 40 to 500 nm and the diameter is usually comprised between 5 and 20 nm. The metallic nanowires are embedded in a polymer matrix (PMMA or polystyrene) with the objective of achieving isolated individual nanowires, which can be structurally oriented in an applied field during the polymerization process. The longer-term motivation is to study not only the static magnetic properties like the magnetization vector inside the wires, but also to investigate the dynamical properties of these quasi-1D systems. SANSPOL experiments on two types of nanowires (long ones and bulky ones) have been performed at room temperature and under a magnetic field (0.5 T) strong enough to align the wire magnetization. A clear magnetic contribution, evidenced by a net difference between *up* and *down* polarisation signals (see figure) is observed. The results are in agreement with a uniform magnetization inside the wires.

[Collaboration: G. Viau, ITODYS Jussieu), T. Maurer, G. Chaboussant, F. Ott, S. Gautrot, LLB]

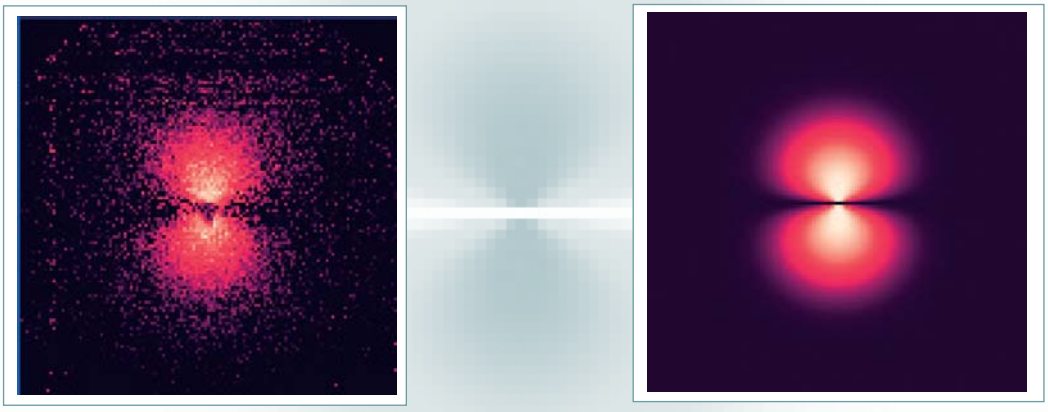

(left): Experimental SANSPOL data ($\Delta I = I^+ - I^-$) of "bulky" nanowires (12 nm diameter and 40 nm length).
(right): Simulation of the magnetic contribution using a uniform magnetic form factor.

[*C11.* V. Garcia] Magneto-structural phase transition in MnAs epilayers grown on GaAs(111)B substrates

MnAs thin films have recently attracted considerable interest due to their growth compatibility with GaAs, and potential applications in spintronics with semiconductors. Bulk MnAs is ferromagnetic in the hexagonal α-phase from low temperature to 313 K where it displays a first-order phase transition to the orthorhombic β-phase. Thin films grown on GaAs(111)B substrates have good crystalline quality with a single epitaxy, atomically sharp MnAs/GaAs interfaces, and smooth surfaces. Also the magnetic phase transition is extended to higher temperature (335 K) in MnAs/GaAs(111)B systems, which is of great interest as the main limitation of MnAs for applications is its low Curie temperature. The evolution of the in-plane and out-of-plane parameters of MnAs epilayers was followed from 100 to 420 K using neutron diffraction (4F1 spectrometer, LLB) to understand the link between structural and magnetic properties in MnAs thin films. The main results from these experiments are summarized in the figure: *(i)* Contrary to bulk material, the mean in-plane parameter is almost constant from 100 to 420 K and follows that of GaAs due to epitaxial strain. *(ii)* This epitaxial strain induces an α-β phase coexistence in a wide temperature range (275–350 K). *(iii)* At low temperature, the α-phase is subject to large in-plane compression but the magnetic moment is close to that of the bulk material (≈ 3.6 μ_B), the β-phase nucleation induces partial relaxation of the ferromagnetic phase up to 350 K, where it disappears. (iv) The unit-cell volume is almost constant before and after the phase coexistence, suggesting that the volume variation is not the leading parameter of the loss of magnetism. We think that the magnetic phase transition could be extended to higher temperature in MnAs epilayers grown on an appropriate substrate having a slightly different in-plane parameter or dilatation coefficient.

[Collaboration: V. Garcia, M. Marangolo, M. Eddrief, INSP, Paris – Y. Sidis, Ph. Bourges, F. Ott, LLB]

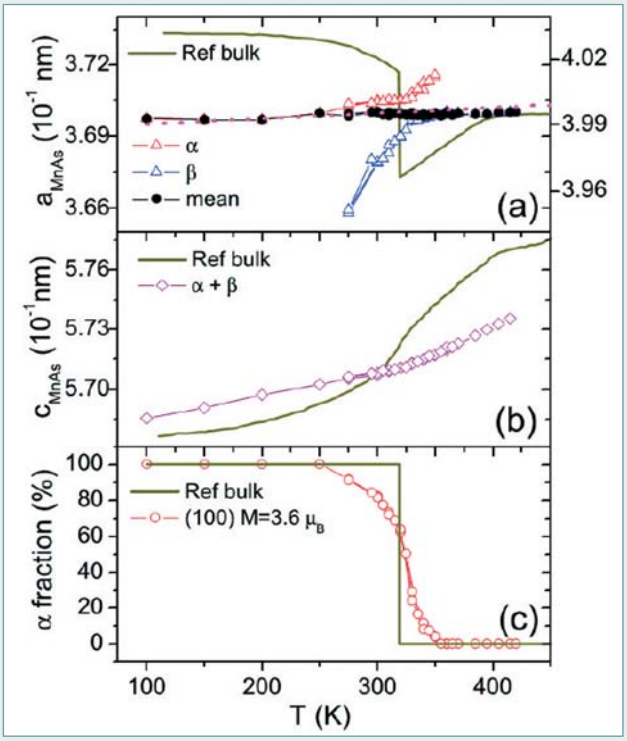

Temperature dependence of structural parameters of a 100 nm thin film of MnAs grown on GaAs(111)B substrate. *(a)*, *(b)* temperature dependence of the in-plane and out-of-plane parameter for both phases deduced from neutron diffraction on MnAs(100) and MnAs(002), respectively. The in-plane and out-of-plane parameters of bulk MnAs are added. *(c)* α-phase fraction deduced from integrated intensity of the spectra along MnAs(100) and considering a constant magnetization per Mn. The mean in-plane parameter calculated from this a-phase fraction, is added in *(a)* together with the evolution of the GaAs parameter.